CHAPTER 1
INTRODUCTION AND LITERATURE REVIEW

1.1. General

The term energy has acquired a new meaning in our day to day life. The energy consumption of any country shows the economic status and living standard of people of that country. Considerable growth in the use of energy has resulted since past few decades due to tremendous boost in industrialization, commercialization, production of goods, increase in service sector etc. Table 1.1 shows the total installed energy generation capacity of India [1] as on 31.03.2013 due to the contribution of different energy sources.

Table 1.1. Total Energy Installed Generating Capacity

Source	**Total capacity (MW)**	**Percentage (%)**
Coal	*130,221*	*58*
Hydroelectricity	*39,491*	*18*
Renewable energy source	*27,542*	*12*
Natural gas	*20,110*	*9*
Nuclear	*4780*	*2*
Oil	*1,202*	*1*
Total	***2,23,344***	

In India, coal based energy generation contributes to approximately 58%, while oil and gas contributes 1% and 9% respectively. Due to the large dependency on fossil fuels usage has resulted in decline in storage of fossil fuels also resulted in increase in fuel import to meet increased energy demand. Another disadvantage of using fossil fuel is that they cause much higher atmospheric pollution, water pollution which is lethal to human health and other species in the ecosystem. Fossil fuels are non renewable and will wipe out from the surface of earth if used indiscriminately. The limited availability of fossil fuels has led researchers to focus on and exploit alternative sources of energy. These include non-conventional energy sources like solar energy, wind energy, tidal wave energy, bio-fuels etc which are gaining popularity nowadays.

India is a developing country and due to its rapid increase in population, inception of various new projects, economic development and expansion of global markets has led to

a substantial increase in energy demand more rapidly and it is expected that the India will become the second largest contributor to global increase in energy market demand. There has been exponential growth in energy demand in different sectors like in industries, domestic, agriculture, commercial, traction etc. Table1.2 shows the total India sector wise electricity consumption with utilities and non utilities as on 31.03.2013 [1].

Table 1.2. Electricity Consumption Sector Wise Utilities and Non Utilities

Sector	**Total Consumption (GWh)**	**Percentage (%)**
Industrial	*3,82,670*	*44.87*
Domestic	*1,85,858*	*21.79*
Agriculture	*1,40,960*	*17.95*
Commercial	*71,019*	*8.33*
Miscellaneous	*44,809*	*5.25*
Traction	*15,431*	*1.81*
Total	***8,52,902***	

There is also a high emphasis on delivering quality power from generating stations to the distribution stations and substations. So the researchers are working on development of automated equipment that is used for controlling the power flow at distant place, fault detection, fault clearing, proper working of relays and circuit breakers, converters, switchgear design etc. To achieve these objectives more effectively and reliably, there is a need to develop, improvise and use new technologies which involve the use of electronically controlled equipment.

With the advent of power electronic devices [2-3] like thyristors, metal oxide field effect transistor (MOSFET), insulated gate bipolar transistor (IGBT), gate turn off (GTO), power diodes etc. The energy scenario has changed at generation, transmission and distribution as well as consumer/utilization level. These devices are used in manufacturing modern control equipment, power converters, inverters, cyclo-converters, personal computers, digital devices, laptops, home appliances, traction drives etc. These equipments inject distortion in current making it non-sinusoidal. Some of these devices are also more susceptible to deviation in power supply, thus power quality issues get complicated further. There are also non linear loads like arc furnaces, electronic loads, adjustable speed drive systems, ac and dc drive, electronically controlled switches which cause distortion in electric power system by injecting currents in addition to fundamental current. They are mainly responsible for poor power factor;

increase in harmonic level which in turn results in high losses in transformer and machines leading to high temperature, saturation, burning etc. hence the overall efficiency of the system decreases. Modern Power system is interconnected. Sometime, a large voltage fluctuations that causes mis-operation of the sensitive equipment results in failure of devices and lead to catastrophic effect in the rest of the electric power system. The overall load on distribution system is seldom balanced and there is no control over the consumer load. So, there is an increase in harmonic level and poor power factor that increase the reactive burden on distribution system. The enhanced use of more sophisticated, controlled and advanced hardware equipment and software for the controlled automation system has increased the concern for power quality issues [4-5]. This has led the power engineers to search for solutions to power quality problems and the entire system more efficient and reliable.

1.2. Power Quality in Distribution System

Utility define power quality in terms of percentage of system reliability statistics [6-8]. For a manufacturer, quality is defined as the working of the equipment without any damage under certain conditions. But as power quality is ultimately concerned with consumer, therefore **Roger Dugan, Mark McGranaghan and Wayne Beaty** in Electrical Power Systems Quality [7] have defined it as "any deviation in voltage, current or frequency of electrical power system that results in false operation or damage to customer devices".

There are various power quality issues that have been defined below:

Harmonics [9] are defined as integral multiples of the fundamental frequency of sinusoidal waveform and thus are the major source of producing distortion in sinusoidal waveform. Due to increased use of non linear equipment like solid state heating controls, electronic ballasts for fluorescent lighting, adjustable speed drives, static UPS, switching mode power supplies in computers, rectifiers, filters, electronic and medical equipments, office electronic machines has resulted in causing more harmonic distortion. These non linear loads distort the sinusoidal current by drawing short burst of current in each cycle or by interrupting current during a cycle. Distorted current produced from harmonic producing loads also distort the voltage as they pass through the system impedance. Extensive use of non linear loads has introduced current and voltage harmonic issues. Harmonic current flowing through impedance result in voltage distortion at the point of common coupling. It results in malfunctioning of the control equipment, and other devices connected in the system. It can cause overheating of

equipment, overloading of capacitor, decreases the efficiency due to increase in the losses owing to the harmonic currents, interference with the communication and control signal, saturation, increase in iron losses and overheating of transformer. Harmonics also results in overheating of power cables and motor rotor experience more heating and pulsated or reduced torque, inadvertent tripping of relays and incorrect measurement of current and voltage by meters. Thus harmonics have detrimental effect on utility and end user equipments.

Faults in distribution or transmission network occur due to failure of equipment, lightning strokes, opening of conductors, damaging windings etc. Sudden change of large load, starting of large load results in decrease of nominal voltage at power frequency for the duration of 0.5 cycle one minute is known as **Voltage Sag**. This cause tripping of circuit breaker and electrochemical relay, malfunctioning of various microprocessor based control systems like programmable logic controller, adjustable speed drive etc leading to stopping process, disconnecting and disrupting the efficiency of the electrical rotating machines.

Short Term Interruption [10] results when there is interruption in electrical supply for duration from few milliseconds to one or two seconds. This is mainly due to faults occurring due to insulation failure, insulator flashover and lightning that causes opening and closing of protection devices to disconnect faulty section of the network. As a consequence, it leads to loss of information and malfunctioning of data processing units, unwanted tripping of protection devices, impact sensitive equipments adversely.

Long Term Interruption occurs when the interruption duration of electrical power becomes greater than one to two seconds. This is caused due to any failure of equipment in electrical power system, storms and objects like tree striking lines or poles, human error, protection devices failure. It results in blackouts and production loss in industries.

Voltage Spikes are defined as very fast change in voltage lasting from several microseconds to few milliseconds. In this short span of time, the voltage value may reach upto thousands of volts. These are due to disconnection of heavy loads, switching capacitors, lightning strokes etc. Such high voltage damages material insulation, electronic components, causes error in data processing units, leading to data loss, and electro-magnetic interference.

Voltage Swell results due to poor voltage regulation during off peak hours, starting and stoping of heavy load resulting in a momentary increase in voltage value at power frequency beyond the normal tolerance. It lasts for duration of more than one cycle or

less than few seconds. This phenomenon is called voltage swell. It leads to loss of processor data, may damage sensitive equipments and cause flickering of screens.

Voltage Fluctuation these are voltage oscillations and modulation of amplitude by signal. This is due to frequent start or stop of electric machines like elevator, arc furnaces, fluctuating load etc. This lead to light flickers causing unsteadiness of visual perceptions which may adversely affects eye sight.

Noise results when high frequency signal is superimposed on the waveform of power frequency. Electromagnetic interference, arc furnaces, electronic equipment, improper grounding, radiations due to welding machines create noise. This causes mal-operation of sensitive equipments, data processing errors, data loss.

Voltage Unbalance in three phase power system is defined as the variation in the amplitude or difference in phase angle. This is due to starting of large single phase loads like induction motor especially under fault. An unbalanced system has negative sequence components that are harmful for all three phase loads.

The above mentioned power quality problems contribute to degrading the quality and reliability of power system. Therefore from customer's point of view it becomes very important to tackle these issues in order to ensure good productivity. On the other hand, electrical utilities want to ensure good quality of power delivered to their customers in today's competitive and deregulated market.

Traditionally passive filters [11] were employed to mitigate harmonics in the system but they had certain disadvantages. They are bulkier in size, more costly and provide limited or fixed compensation for reactive power. They are also more prone to resonate with the system impedance leading to abnormal conditions in the electrical system. Innovative technologies are now available which are cost effective also. The custom power devices are used in distribution systems for enhancing the reliability and quality of the power supply.

1.3. Power Quality Solutions

The concept of custom power devices (CPD) was proposed in 1988 by **Dr. N. G. Hingorani** [12]. It represents an emergence of new technology targeting at enhancing power supply reliability and power quality by using advanced and new technologies, such as power electronics technology, microprocessor technology and control technology in mid and low voltage power supply and distribution system. The Custom Power devices offer a new way to resolve power quality problems in distribution system.

1.3.1. D-STATCOM

D-STATCOM is a shunt compensator that is connected in parallel at load side. The concept of shunt active filter was first introduced by **Gyugyi and Strycula** in 1976 [13]. A basic configuration of shunt active filter is shown in the Fig.1.1. A shunt compensator helps to maintain unity power factor and since line current contains only positive sequence component for a given load and therefore line losses are also reduced by injecting the required amount of current in phase opposition of the load current. It enables better utilization of distribution system. There are various control algorithms proposed by different author to mitigate power quality issues.

H. Akagi [14-15] has introduced Instantaneous Reactive Power Theory (IRPT) for reactive and harmonic current detection. It is seen that IRPT implementation works effectively for voltage regulation, harmonic and reactive power compensation. However, there may be an error in calculating reference signal if the source voltage is highly unbalanced.

C.L. Chen and C.E. Lin [16] shows the implementation of Synchronous Reference Frame Theory (SRFT) transforms where, three-phase quantity into two phase quantity d-q frame and vice-versa. This leads to computational delay due to the presence of complex mathematical transformation.

B. Singh and S. Kumar [17-21] has reported a comprehensive study of an overview of active power filter and their different topologies. A new control technique known as unit template technique has been developed and implemented in different configurations. This technique extracts the unit templates from the source voltage and does not require any mathematical transformation. Power balance theory without using phase locked loop for generating unit templates has been discussed to extract reference current to mitigate power quality issues.

Vishal Verma [22-23] discussed the design and implementation of an indirect current control of a parallel hybrid filter (PHF) system with rectifier load to eliminate generated harmonics. The proposed control enhances the performance of the passive filters (PFs) under unbalanced situations that are existing in the PFs under fault conditions.

Y. Li, K. H. Ng and G. C. Y. Chong [24] shows that PI controller has the advantage that it follows the set point excellently and has good disturbance rejection tendency at appropriate gain cross over frequency. It also has some demerits such as it increases the overall system gain and saturates the integral term that may lead to instability. These controllers sometimes does not give satisfactory results, if system parameter or

condition changes. Therefore new adaptive controller is developed using neural network theory providing adaptive filtering.

Chen and O'connell [25] proposed neural network algorithm using back propagation technique for estimating the harmonic. But using neural network requires offline data training for specific loading conditions. Therefore it does not provide appropriate results with other loading conditions.

Widrow, McCool, Larimore, and Johnson [26-27] has shown another method for online determination of compensating signal which is least mean square algorithm based on Adaline algorithm.

B. Singh, V. Verma and J. Solanki [28-30] presented neural network technique for extracting the positive fundamental current with non linear load when the source side voltage is distorted.

S. Karanki, N. Geddada, Mahesh K. Mishra, and B. Kumar [31] has presented D-STATCOM topology that reduces DC link voltage rating.

M. Suresh and A. K. Panda [32] has discussed about fuzzy logic controller. Mamdani type fuzzy controller is used for voltage regulation at DC bus voltage. it has been interfered that fuzzy is easy to understand, implement and robust to the system. The dynamic response of fuzzy logic controller is good than PI controller.

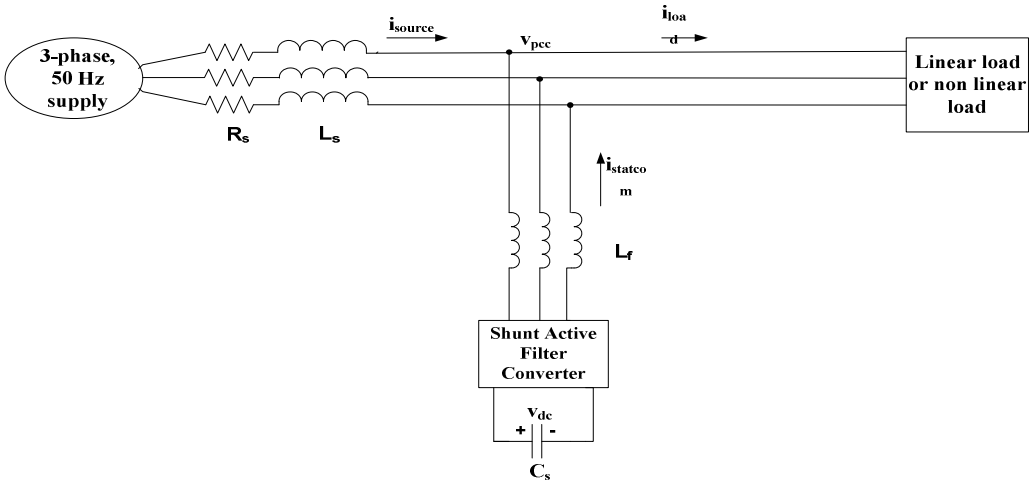

Fig. 1.1. Block diagram of D-STATCOM system

1.3.2. DVR

Dynamic voltage restorer is a series connected active filter which injects the required compensating voltage into the system through transformer for eliminating voltage disturbances at source side. It is basically a dual of shunt filter. Fig. 1.2 shows the basic block diagram of DVR.

There are different topologies reported in the literature. DVR mitigates the power quality problems mainly generated at the load terminal due voltage and current disturbances at the source side and compensates for voltage harmonics. A DVR maintains the voltage constant at the load terminal during voltage dip and voltage swell conditions. DVR does not compensate harmonics at load terminal but acts as an isolator for the current harmonics coming from the source end. It provides high impedance path for the harmonics thus restricting it at source side and safeguarding filters at load side.

B. Bhavaraju and N. Enjeti [33] has proposed the different filter scheme based on operating principle, compensation performance and control scheme. The scheme is used for only voltage compensation.

S. Bhattachrya and D. Divan [34] has discussed synchronous reference frame algorithm based implementation of series hybrid configuration to mitigate power quality problems.

Nielsen, Blaabjerg and Mohan [35] has discussed different topologies for DVR control and their performance has been analyses for mitigating voltage sag conditions.

Ghosh, Jindal and Joshi [36] has described the designing of capacitor connected at DVR to provide sufficient energy for unbalance and distorted load condition.

Weiliy and Newman [37-38] presented the robust control scheme for DVR control at medium voltage level and selective compensation.

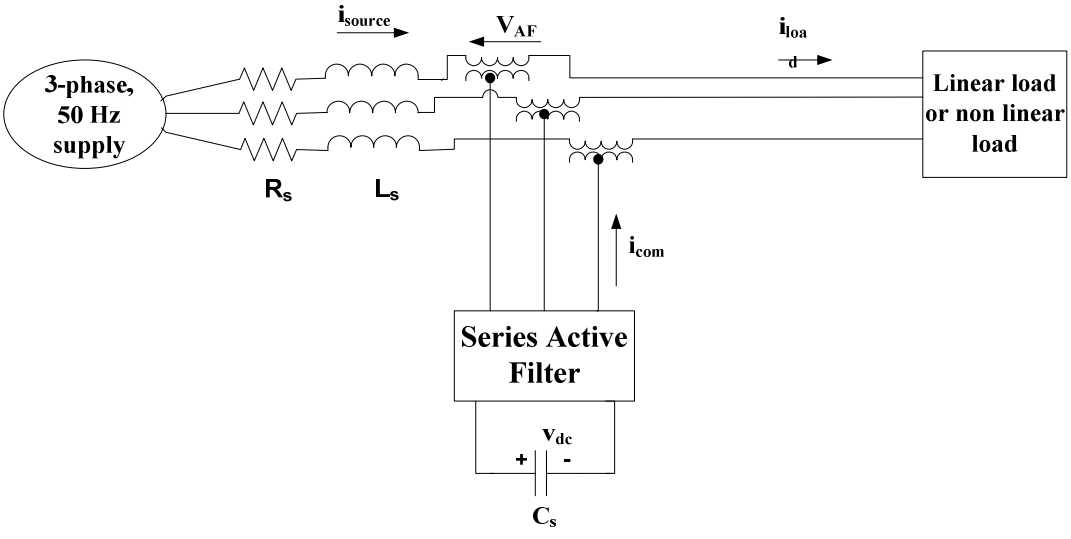

Fig. 1.2 Block diagram of DVR system.

1.3.3. UPQC

There are several demerits in using shunt and series active filters separately as a compensating device. A D-STATCOM filters successfully current harmonics at the load end and provides reactive demand. However, in general the terminal voltage is always distorted, which is used for computation of reference currents. Therefore a shunt compensator is not able to provide compensation properly if supply side voltage is distorted, which is generally the case.

DVR also has limitations that it provides compensation only when the source is distorted and load is linear. But if the load is non-linear, there is presence of distortion at the load side. So there is some distortion present in current that will create voltage drop at two sides of serial transformer. So it becomes difficult for series compensator to detect and compensate.

In some cases, nonlinear loads on one hand inject harmonics into the system but on the other hand, they themselves demand a good power quality supply. Hence the concept of unified power quality conditioner (UPQC) arises to compensate for both current and voltage disturbances. In UPQC, both series and shunt active compensators are incorporated to compensate for the demerits caused by the series and shunt active filter. Fig.1.3 shows the basic block diagram of UPQC. DC link is realized using DC capacitor which is common to series and shunt converters and also maintains the DC link voltage. Inductor (L_f) is used to shape the compensating current. The series converter is connected to the network through the series injection transformer with suitable ratio to reduce current or voltage rating of series converter.

B. Singh [39-40] has described UPQC can be used for improving power quality problems such as voltage sag, unbalance, and flicker, as well as harmonics, dynamic active and reactive power regulation. The DC bus voltage is regulated by shunt converter while DVR supplies the required energy to the load in case of transient disturbances in source voltage.

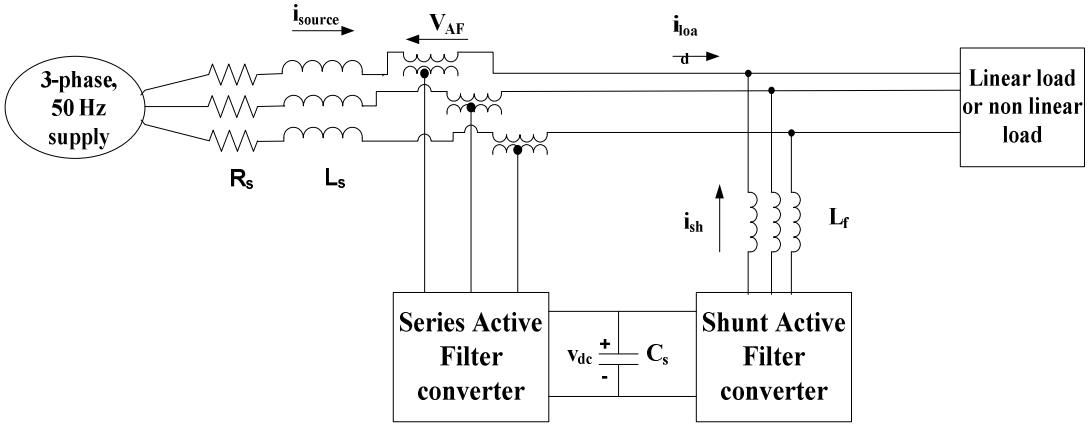

Fig. 1.3. Basic block diagram of UPQC system

1.4. Trends in Power Quality Standards

It is important to formulate standards that can tackle power quality issues and reduce the severity of harmonics which affect the performance of sensitive equipments. Deregulation practices have also increased the need of standardization so that offending organization can be held for penalty and or fixing the problems. IEC and IEEE standards [41-42] are the primary standards to be met by power system to ensure quality. In addition, there are also other power quality standards organizations such as IEEE-519, IEC 61000, EN 50160. IEEE has developed IEEE standards 1159-1995 copyright [43], recommended Practices for Monitoring Electric Power Quality so that power quality industries can compare their measurement results taken from different instruments. This standard define various power quality terms and categorize IEEE standards for various power quality topics such as surge protection, grounding, harmonics, fire safety/life, disturbances, mitigation equipments, telecommunication equipments, utility interface, monitoring, noise control, load immunity and system reliability. IEEE 519 1992 copyright related to recommended practices and requirements for harmonic control in electric power systems. This recognizes that primary source of harmonic current is non linear loads located on the utility customer or end user side of the meter. Utility may also transmit harmonic voltage to the end user due to amplification of harmonic voltage utility. IEEE 519-1992 defines harmonic limits on end user side of the meter as total distortion demand (TDD) and on utility side of meter as total harmonic distortion (THD). IEEE 519-1992 defines harmonic limits on end user and utility side.

These standards are not permanent and get updated by expert's knowledge. There are improvements in the measuring instruments and analytical techniques that taken into account for ensure best standard practices.

1.5. Conclusion

The proliferation of automation industry with high power electronic based controllers has led to new studies focusing on power quality issues. Various power quality problems have been discussed in this chapter. Conventional solutions in the form of passive filters have been used but they have their own shortcomings. Custom power devices offer new solutions to power quality problems and an exhaustive literature review on D-STATCOM, DVR, UPQC is presented in this chapter. Configuration and control techniques for these devices are reviewed. Finally some commonly used standards are discussed which play important role in recommending standard practices for mitigating power quality problems.

CHAPTER 2
CONVENTIONAL CONTROL TECHNIQUES FOR D-STATCOM

2.1. General

Last chapter gives an overview of power quality problems, its causes and solutions. In this chapter, two conventional control schemes viz synchronous reference frame theory (SRFT) and power balance theory (PBT) for distribution static compensator (D-STATCOM) have been discussed in detail. Fast processing and proper functioning of shunt active filter depends on the type of control scheme used for generating the proper reference signals. Any control algorithm involves proper sensing of current and voltage signals using current and voltage sensors. The computation of compensating current or voltage signals mainly depends on the control algorithm used and type of topology used in designing active filter. The gating signals are generated for voltage source converter of active filter using PWM or current hysteresis controller. Various control algorithms have been reported in the literature. The control algorithm based on time domain senses the instantaneous current or voltage signals to derive the compensating signals. There are various control algorithm mentioned in the literature such as SRFT (Synchronous Reference Frame Theory), instantaneous active- reactive power theory, power balance theory (PBT), neural network theory, notch filter theory, adaptive filter theory, fuzzy logic, neuro-fuzzy logic. In this chapter, a comparative study for SRFT and PBT has been carried out and the model has been developed in MATLAB environment using Sim Power System (SPS) toolbox. The simulation results are taken for both the control schemes with non linear loads with both the schemes.

2.2. System structure

Fig. 2.1 shows the system structure of D-STATCOM. A three-phase source of line to line 110V (rms) is used as electrical power supply with very low source impedance. A three-leg voltage source converter is used as D-STATCOM and it is connected to point of common coupling (PCC) through inductors. These inductors reduce ripples during switching. The voltage source converter consists of six insulated gate bipolar transistor (IGBT) switches along with anti parallel diode. D-STATCOM is made self supported by connecting a DC capacitor at its DC side. A small amount of real power current is required to replenish internal losses of VSC and keep the voltage across capacitor at

desired voltage which is controlled through PI controller. This PI controller compensates for the power losses in the converter by comparing reference voltage to actual voltage across the capacitor. A three phase diode rectifier with *RL* load at the output of the rectifier is used as non linear load. The switching signals for the VSC can be computed depending on the type of control algorithm used for computation. An indirect current control method is used for generating switching signals for VSC and this is based on computation of slowly varying source currents. The reference source currents are derived by sensing the load currents and dc link voltage. These reference currents are obtained, then compared with the actual source currents through hysteresis current controller and switching pulses are generated.

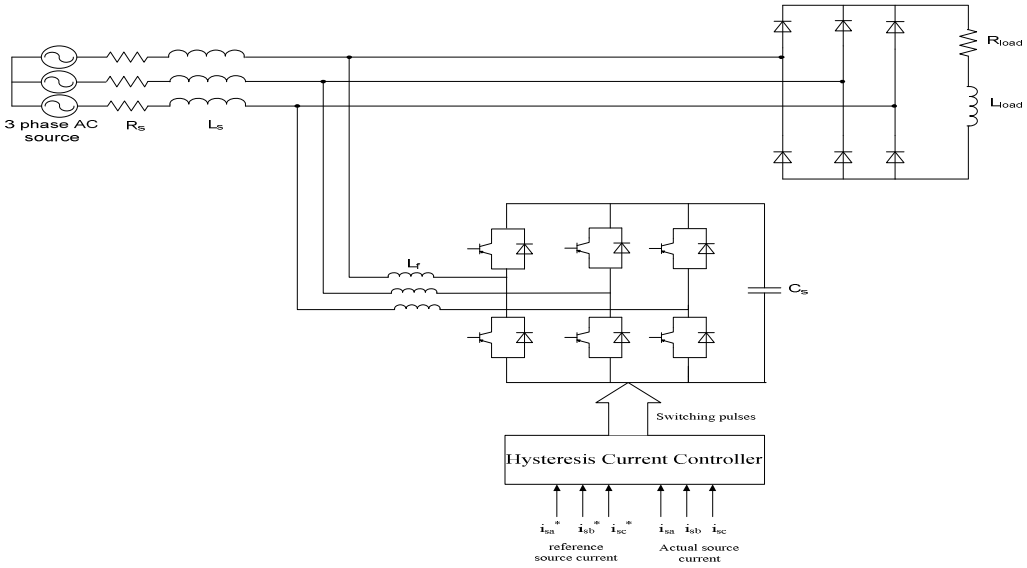

Fig. 2.1. System structure of D-STATCOM

2.3. Hysteresis Current Controller

Carrier less pulse width modulation (PWM) hysteresis current controller (HCC) is most commonly used current controller to obtain switching pulse generation for D-STATCOM by comparing reference current with actual current. HCC is simple, robust and have good dynamic performance which makes it more attractive choice. There is a hysteresis band which lies between $i_{sr} + h$ and $i_{sr} - h$ region for a hysteresis band of value *'h'*. If the source current exceeds the upper limit band ($i_{sr} + h$) then the current is decreased by applying negative voltage by switching on lower switch. Similarly, when current drops below lower limit, then the current is increased by applying the positive voltage by

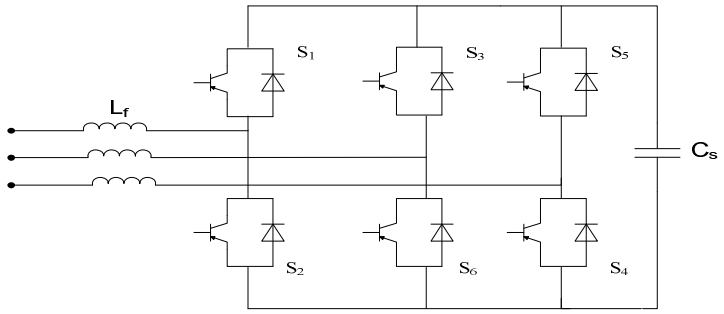

Fig. 2.2. Switching sequence of D-STATCOM

switching on upper switch. Thus the current remains within the band 'h' and switching gating signals are generated.

Fig. 2.2 shows switching sequence of the inverter. The switching of the inverter is developed using following logic for three legs.

$$u_a = \begin{cases} 1, & when\ S1\ is\ ON \\ -1, & when\ S4\ is\ ON \end{cases} \quad (2.1)$$

$$u_b = \begin{cases} 1, & when\ S3\ is\ ON \\ -1, & when\ S6\ is\ ON \end{cases} \quad (2.2)$$

$$u_c = \begin{cases} 1, & when\ S5\ is\ ON \\ -1, & when\ S2\ is\ ON \end{cases} \quad (2.3)$$

In hysteresis current controller (HCC), the current remains inside the band but as the band width is narrowed consequently the actual waveform becomes closer to the reference waveform but contrary the switching frequency will be higher. Hence in hysteresis current controller the switching frequency remains unknown factor. Constant switching frequency reduces the undesired stress on semiconductor devices. Therefore, various schemes have been reported to reduce the switching frequency and to maintain constant switching frequency. **T.W. Chun and Choi** [43] have developed a constant switching frequency current controller. **B.K. Bose** [44] has introduced an adaptive hysteresis based current control technique of voltage fed PWM inverter for machine derive system by tracking the current in hysteresis band.

2.4. d-q theory control scheme

Fig. 2.3 shows the block diagram of Synchronous Reference Frame Theory (SRFT) based controller. SRFT is a method for extracting the reference current by mathematical transformation

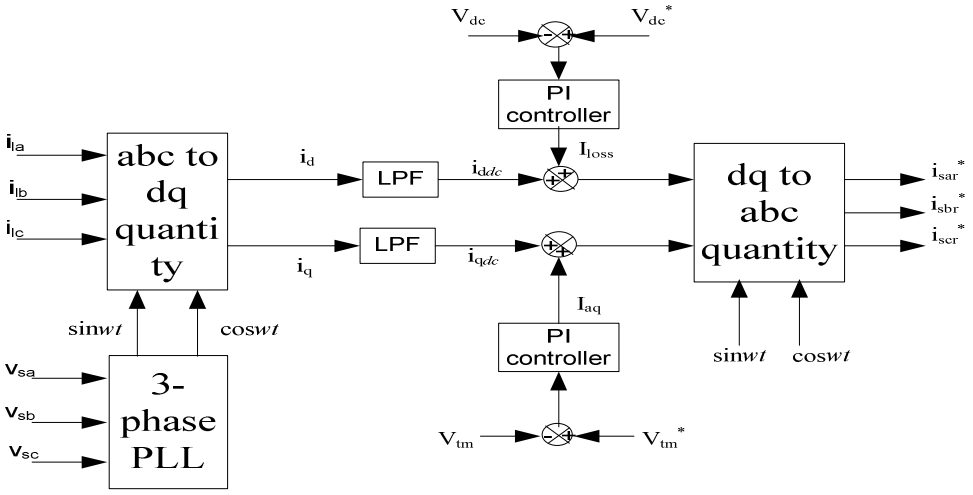

Fig. 2.3. Block diagram of SRFT control scheme.

of three-phase quantities (either voltage or current) into direct-quadrature-zero (dq0) quantities to simplify the three phase analysis. In case of balanced three phase circuit, dq0 quantity reduces three AC quantities into two DC quantities which rotate with synchronous speed. Simplified calculations can then be carried out on these imaginary DC quantities before performing the inverse transform to recover the actual three-phase AC quantities.

Equation (2.4) uses transformation matrix for converting any three phase (*abc*) signal either voltage or current quantity into *dq0*, where [T] is the transformation matrix and α is the angle between *d*-axis and *q*-axis. '*u*' can be either be voltage signal or current signal.

$$u_{dq0} = [T]*u_{abc} = \sqrt{\frac{2}{3}}\begin{bmatrix} \cos\alpha & \cos(\alpha-\frac{2\pi}{3}) & \cos(\alpha+\frac{2\pi}{3}) \\ sin\alpha & \sin(\alpha-\frac{2\pi}{3}) & \sin(\alpha+\frac{2\pi}{3}) \\ \frac{\sqrt{2}}{2} & \frac{\sqrt{2}}{2} & \frac{\sqrt{2}}{2} \end{bmatrix}\begin{bmatrix} u_a \\ u_b \\ u_c \end{bmatrix} \quad (2.4)$$

For converting *dq0* quantity into three phases (*abc*) quantity equation (2.5) is used, where $[T]^{-1}$ is the inverse transformation matrix.

$$u_{abc} = [T]^{-1}*u_{dq0} = \sqrt{\frac{2}{3}}\begin{bmatrix} \cos\alpha & sin\alpha & \frac{\sqrt{2}}{2} \\ \cos(\alpha-\frac{2\pi}{3}) & \sin(\alpha-\frac{2\pi}{3}) & \frac{\sqrt{2}}{2} \\ \cos(\alpha+\frac{2\pi}{3}) & \sin(\alpha+\frac{2\pi}{3}) & \frac{\sqrt{2}}{2} \end{bmatrix}\begin{bmatrix} u_d \\ u_q \\ u_0 \end{bmatrix} \quad (2.5)$$

The *dq0* transformation is the projection of three phase quantities rotating with some angular velocity into two DC components rotating with same angular velocity as three

phase quantity. The axis which is in phase with actual axis is called direct axis or d-axis and the axis which 90^o phase shifted from d-axis is called quadrature axis or q-axis. Since the system is three phase without neutral wire therefore the *0*-axis will be absent.

2.4.1. D-STATCOM Operation for Power Factor Improvement

Three phase load current is sensed through sensors and transformed into dq0 component using equation (2.4). The angle of three phase source is estimated by using phase locked loop (PLL) from the ideal balanced voltage source. This phase angle is used in transformation equation. Then, '*d*' and '*q*' components of the load current are obtained. Since the system is three-phase, three-wire system with no neutral point, therefore no zero-component is present. For obtaining unity power factor operation, only d-component of the load or the in-phase component along with loss component in inverter to derive the reference supply current. The loss component can be obtained by controlling the DC link voltage through PI controller. The sensed DC voltage is compared with the reference DC link voltage to generate the error and it is passed through PI controller. The output of PI controller is obtained as shown in equation (2.6).

$$i_{loss(n)} = i_{loss(n-1)} + k_p \{V_e - V_{e(n-1)}\} + k_i V_{e(n)} \quad (2.6)$$

where k_p and k_i are the proportional and integral gains of the PI controller. $V_{e(n)}$ is the error in dc link voltage at 'nth' interval. $V_{e(n-1)}$ is the error in DC link voltage at (n-1)th interval. The reference source current obtained for unity power factor operation as shown in equation (2.7), where $\bar{\imath d}$ is the DC component of *d*-axis obtained from low pass filter.

$$i_{dref} = \bar{\imath d} + i_{loss} \quad (2.7)$$

$$i_{sabc}^{*} = T^{-1}\begin{bmatrix} i_{dref} \\ 0 \end{bmatrix} \quad (2.8)$$

Reverse transformation is applied to obtain three phase reference source current as shown in equation (2.8). The reactive power demanded by load is locally fed by D-STATCOM hence the '*q*' component of the reference supply current is taken as zero. This will make source current in phase with PCC voltage.

2.4.2. D-STATCOM operation for Voltage Regulation

In this case, the voltage at PCC is regulated through PI controller at AC side by comparing the reference voltage and actual voltage at PCC, the output obtained is shown in equation (2.9).

$$i_{aq(n)} = i_{aq(n-1)} + k_p' \{V_{ae} - V_{ae(n-1)}\} + k_i' V_{ae(n)} \quad (2.9)$$

where $V_{ae(n)}$ is the error between the sensed AC voltage and actual AC voltage at point of common coupling at nth interval whereas $V_{ae(n-1)}$ is error at (n-1)th interval. k_p' and k_i' are the proportional and integral gain of PI controller. The reference current is calculated as shown in equation (2.10).

$$i_{qref} = i_{aq} - \bar{\imath_q} \quad (2.10)$$

where i_{aq} is the current required to maintain the AC voltage at PCC and $\bar{\imath_q}$ is the DC component extracted by filtering through low pass filter. The three-phase reference source currents are calculated using equation (2.11).

$$i_{abc}^{*} = T^{-1}\begin{bmatrix} i_{dref} \\ i_{qref} \end{bmatrix} \quad (2.11)$$

2.5. MATLAB based model and Simulation results

Fig. 2.4 shows the SRFT model developed in MATLAB environment using Simulink and Sim Power System toolboxes. Simulation results are taken to prove the validity of control algorithm.

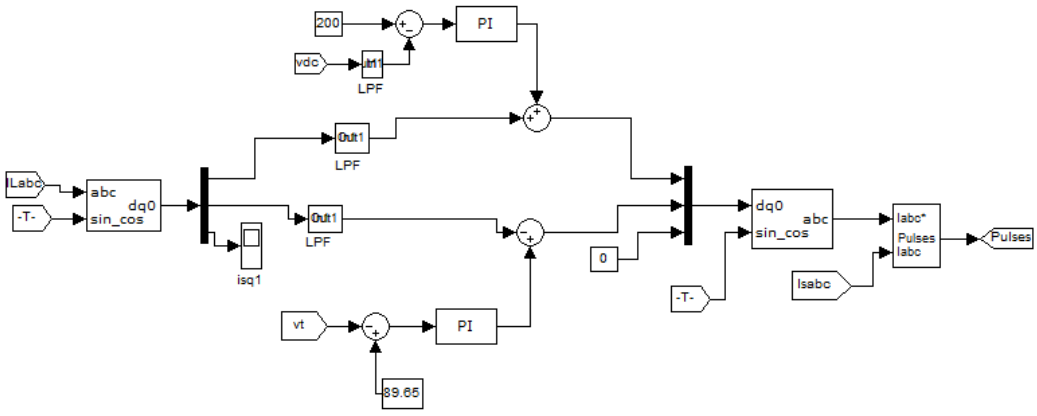

Fig. 2.4. MATLAB model based on SRFT control algorithm

2.5.1 Result for power factor improvement

Fig. 2.5 shows the results with non linear load under steady state and unbalanced conditions. It is observed that DC link voltage attains a reference voltage 200V once D-STATCOM is connected to the system. Fig. 2.6. show the plot of d-component of reference current (i_{dref}) including the loss component under steady state condition. Source currents become sinusoidal and in-phase with voltage is shown in Fig. 2.7. It is observed that the compensator eliminates harmonics from the source current and THD in source current is found to be 1.53% as shown in Fig. 2.8. The load current THD is 27.26% as shown in Fig.2.9. At t=0.3 secs phase 'c' has been removed and the load current of phase 'c' (i_c) becomes zero. It is observed that there is a sudden voltage rise when load is removed at t=0.2secs however by controller action, the DC link voltage reverts back to its reference value of 200V. At t=0.4 secs, phase 'c' is reconnected, there is voltage dip in DC link voltage and it regain its reference value of 200V by the action of PI controller.

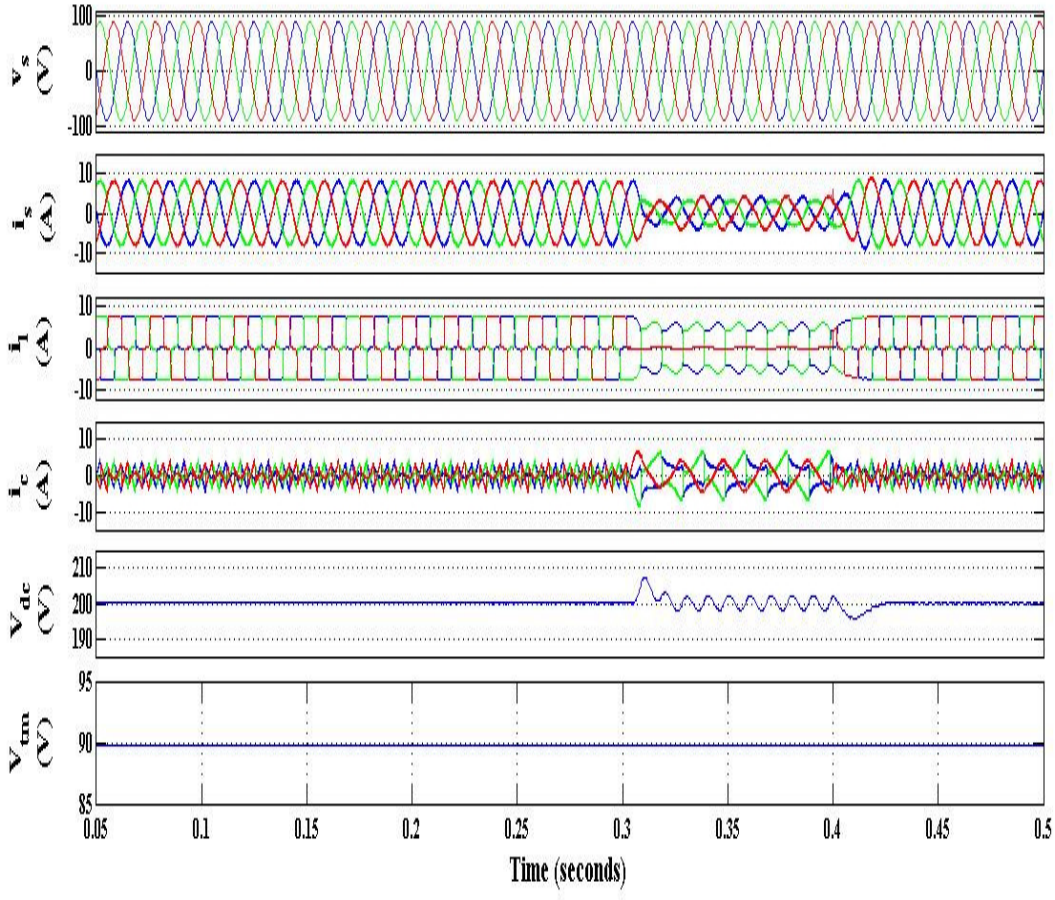

Fig. 2.5.Waveform of source voltage (v_s), source current (i_s), compensator current (i_c), load current (i_l), dc voltage V_{dc}, terminal voltage (V_{tm}) under steady state /unbalance conditions (UPF mode)

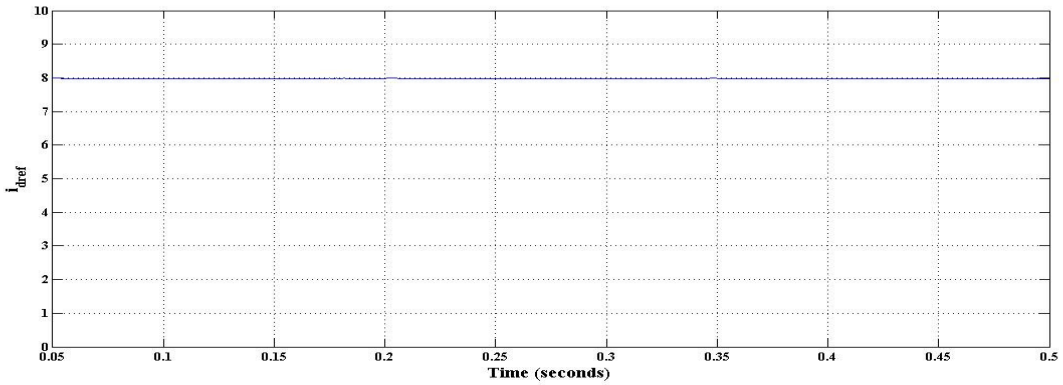

Fig. 2.6. Plot of d-component (i_{dref}) of reference current under stedy state condition

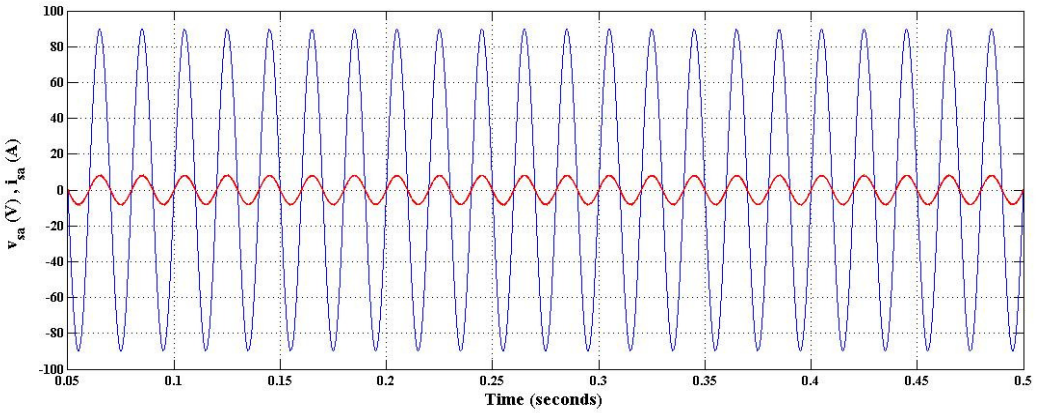

Fig. 2.7. Source voltage (v_{sa}) and Source current (i_{sa}) waveform

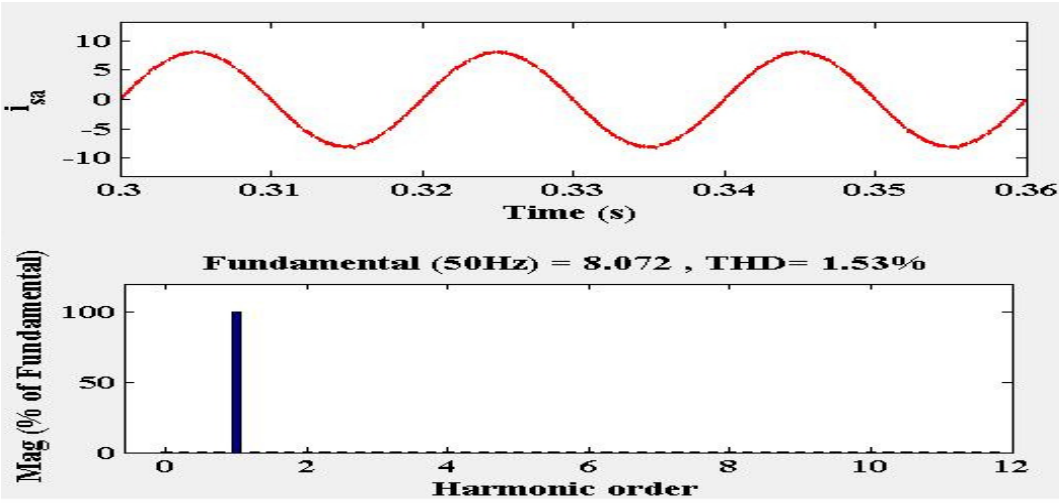

Fig. 2.8. Waveform and THD for source current (i_{sa})

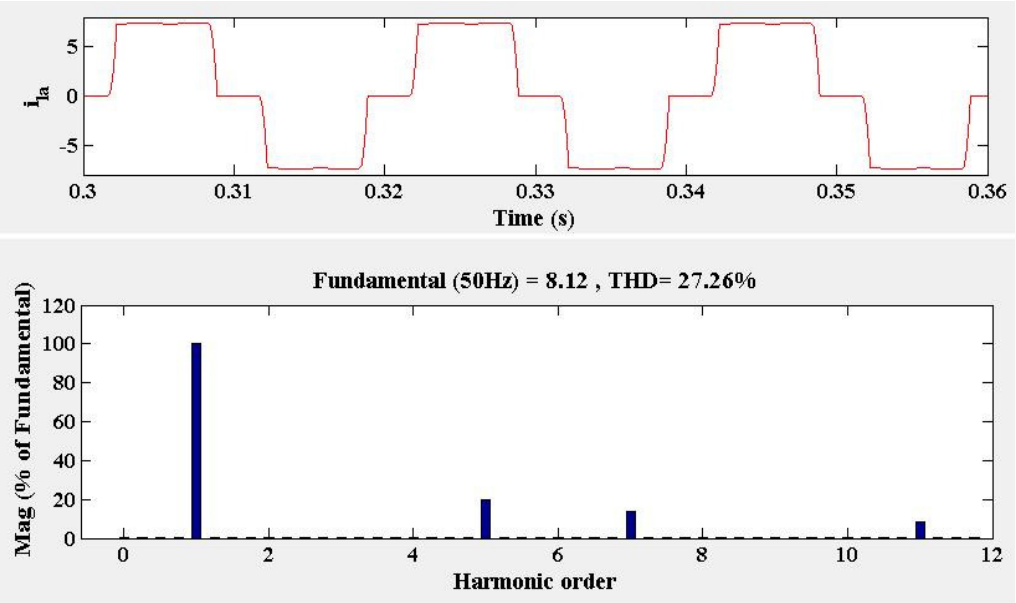

Fig.2.9. Waveform and THD of load current (i_{la})

2.5.2. Results for Voltage Regulation

Fig.2.10 shows the results for voltage regulation at point of common coupling under steady state / unbalanced conditions with non linear load. It is observed that the control algorithm is able to maintain PCC voltage to its reference voltage of 89V very quickly. The source current becomes sinusoidal even though the load current contains harmonics. With the SRFT algorithm, the reference source currents are calculated as shown in equation (2.4) to (2.11). Whether, we use the indirect current control scheme for calculation of reference source current or the calculation of reference compensator current using direct current control method, both the schemes work fairly. The compensator injects the required current for harmonic elimination. Fig. 2.11 shows the plot of q-component (i_{qref}) of reference current under steady state condition. Fig. 2.12 and Fig. 2.13 show that the THD of source current waveform is 1.39% when load current waveform has THD of 27.24%. Thus the compensator eliminates harmonics at source side even under the presence of

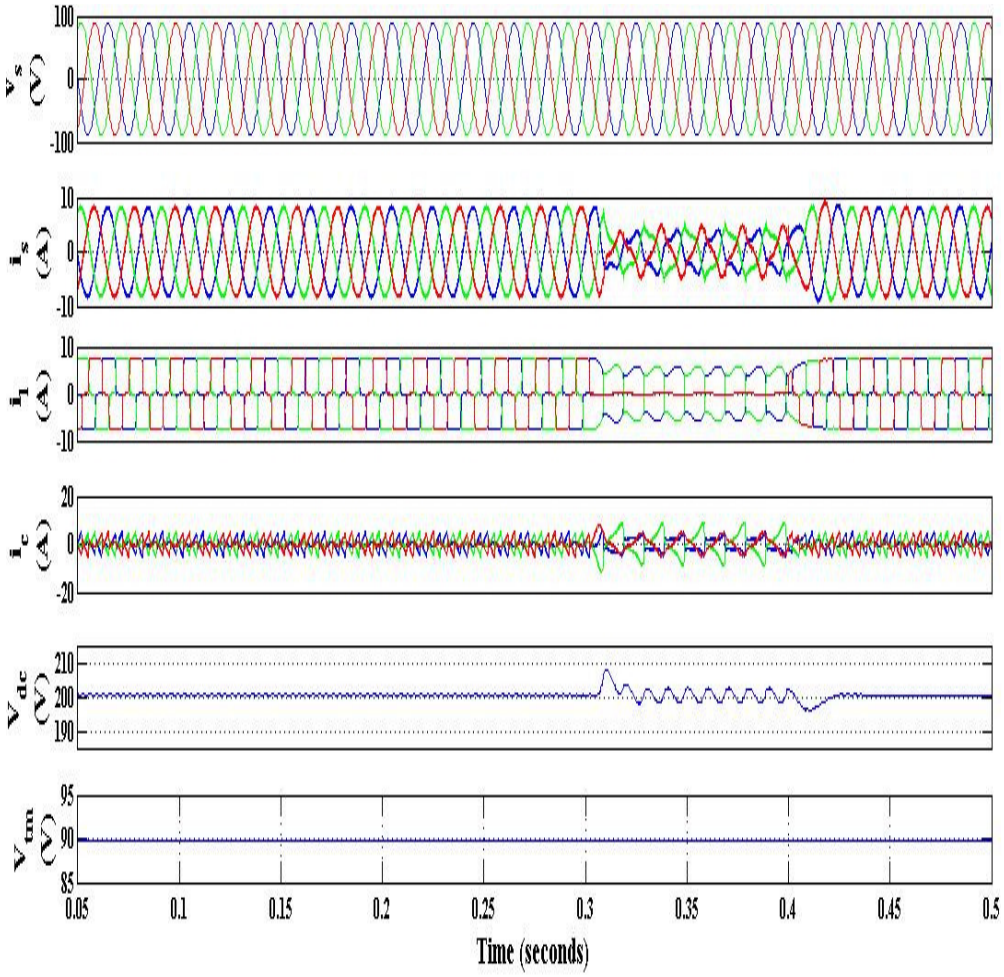

Fig. 2.10. Waveform of source voltage (v_s), source current (i_s), compensator current (i_c), load current (i_l), DC voltage (V_{dc}) and terminal voltage (V_{tm}) (voltage regulation mode)

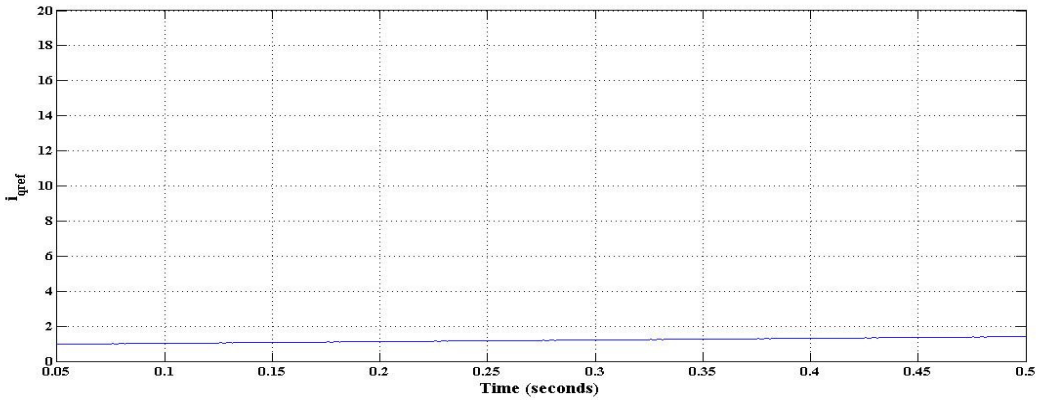

Fig. 2.11. Plot of q-component (i_{qref}) of reference current under steady state condition

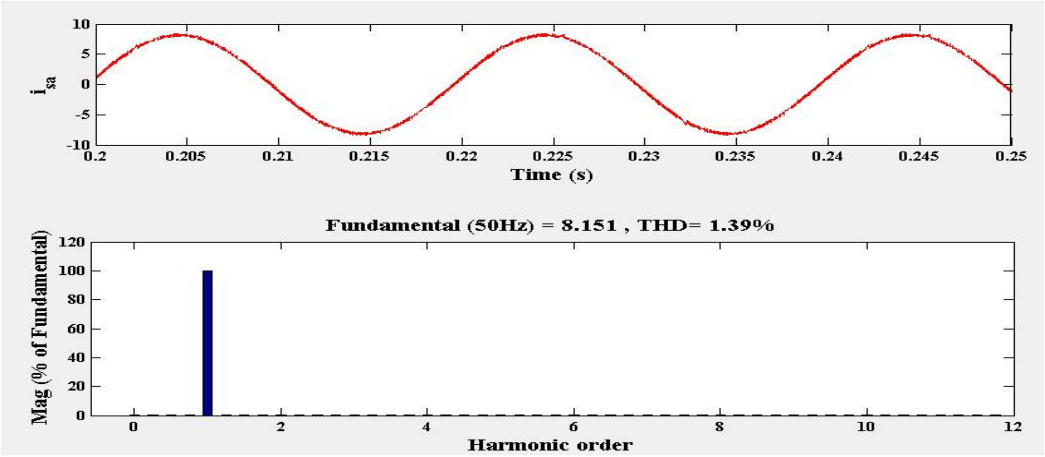

Fig. 2.12. Waveform and THD of source current (i_{sa})

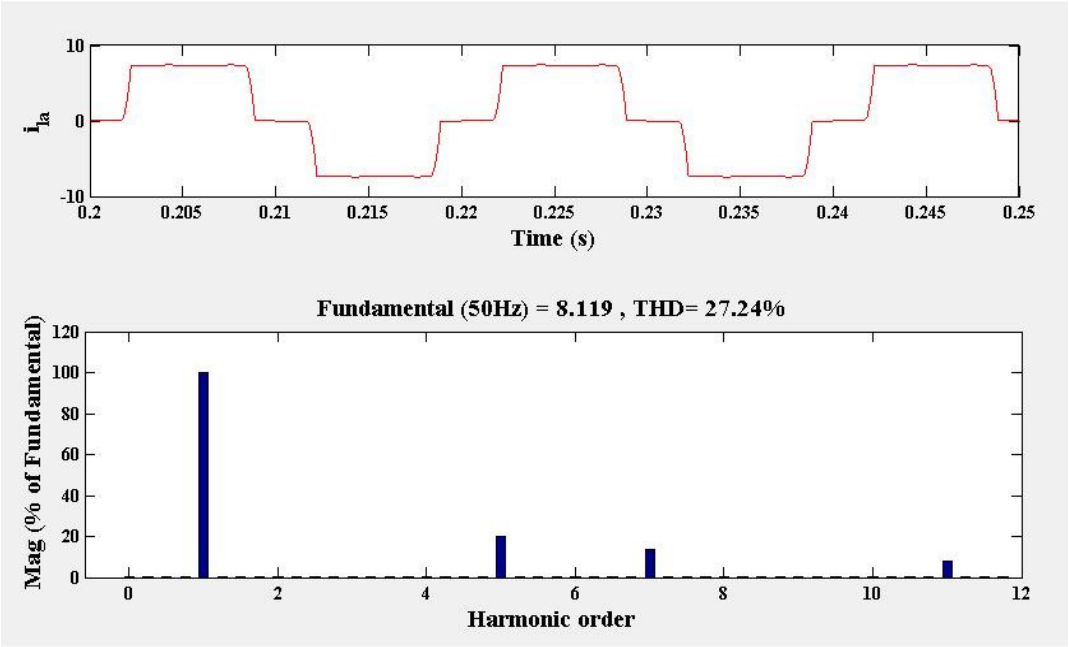

Fig. 2.13. Waveform and THD of load current (i_{la})

2.6. Power Balance Control Scheme

The control algorithm used for distribution static compensator is based on power balance theory is shown in Fig. 2.14. The reference currents are extracted by sensing the load current ($i_{la,}$ $i_{lb,}$ i_{lc}), load voltage ($v_{la,}$ $v_{lb,}$ v_{lc}), source voltage ($v_{sa,}$ $v_{sb,}$ v_{sc}), source current ($i_{sa,}$ $i_{sb,}$ i_{sc}), dc link voltage (V_{dc}), voltage at PCC (V_{tm}) through current sensors and voltage sensors.

The amplitude of PCC voltage is calculated from equation (2.12).

$$V_{tm} = \sqrt{\frac{2}{3}\left(v_{ta}{}^2 + v_{tb}{}^2 + v_{tc}{}^2 \right)} \qquad (2.12)$$

where, v_{ta}, v_{tb} and v_{tc} are terminal voltages at point of common coupling.

Unit vector templates in phase with PCC voltage are obtained from the equation (2.13).

$$u_a = \frac{v_{sa}}{v_{tm}} \quad ; \quad u_b = \frac{v_{sb}}{v_{tm}} \quad ; \quad u_c = \frac{v_{sc}}{v_{tm}} \tag{2.13}$$

Unit vectors in quadrature with the PCC voltage are obtained from the equation (2.14a), (2.14b) and (2.14c).

$$w_a = (u_c - u_b)/\sqrt{3} \tag{2.14a}$$

$$w_b = u_a/\sqrt{2} + (u_b - u_c)/\sqrt{6} \tag{2.14b}$$

$$w_c = (u_b - u_c)/\sqrt{6} - u_a/\sqrt{2} \tag{2.14c}$$

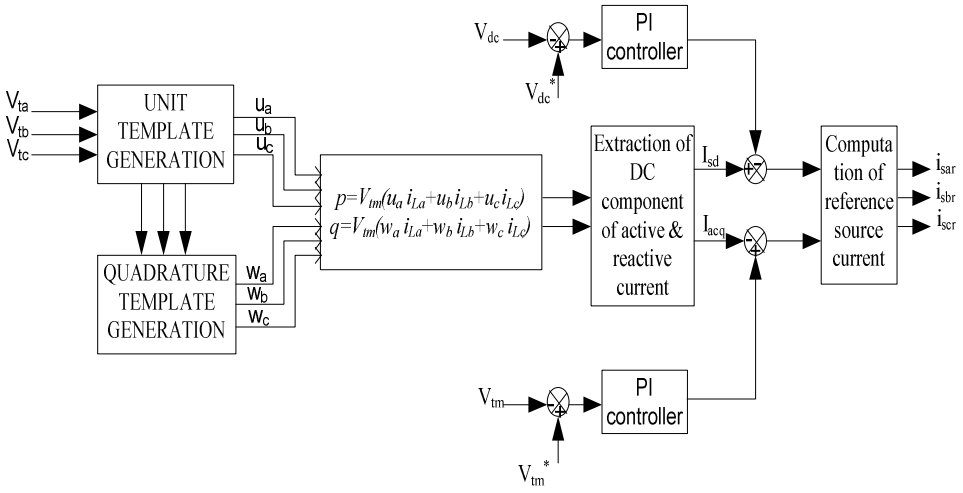

Fig. 2.14. Block diagram of PBT control scheme

The instantaneous active power (p_{load}) and reactive power (q_{load}) are calculated from equation (2.15a) and (2.15b5).

$$p_{load} = V_{tm} \times (u_a\, i_{La} + u_b\, i_{Lb} + u_c\, i_{Lc}) \tag{2.15a}$$

$$q_{load} = V_{tm} \times (w_a\, i_{La} + w_b\, i_{Lb} + w_c\, i_{Lc}) \tag{2.15b}$$

The calculated load power has two components. The first one is the DC component and second one is AC component is shown in equation (2.16a) and (2.16b). The DC component is extracted by filtering the load power through low pass filter (LPF).

$$p_{load} = \overline{p} + \tilde{p} \tag{2.16a}$$

$$q_{load} = \overline{q} + \tilde{q} \tag{2.16b}$$

For obtaining the power factor correction, it is assumed that source supplies the load active power (p_{load}) and power loss (p_{loss}) in the converter. The reactive power requirement of the load is fed locally from distribution static compensator. The DC

component ($\overline{p}$) of load active power is extracted by filtering it through low pass filter from which required active load current (I_{sd}) is calculated as shown in equation (2.17).

$$I_{sd} = \frac{2}{3} \times \frac{\overline{p}}{V_{tm}} \tag{2.17}$$

For the regulation of DC link bus voltage (V_{dc}), a PI controller is employed. The output of this PI controller is considered as loss component of power in the converter is shown in equation (2.18).

$$i_{loss(n)} = i_{loss(n-1)} + k_{pd} \{V_{de} - V_{de(n-1)}\} + k_{id} V_{de(n)} \tag{2.18}$$

where, $V_{de(n)} = V_{dcr} - V_{dc(n)}$ denotes the error between sensed DC voltage and reference DC voltage. k_{pd} and k_{id} are proportional and integral gains of DC bus voltage PI controller.

The amplitude of active power component of the reference source current is calculated from equation (2.19), (2.20a), (2.20b) and (2.20c) by adding I_{sd} and i_{loss} components.

$$i_{sdr} = I_{sd} + i_{loss} \tag{2.19}$$

$$i_{sdar} = u_a \times i_{sdr} \tag{2.20a}$$

$$i_{sdbr} = u_b \times i_{sdr} \tag{2.20b}$$

$$i_{sdcr} = u_c \times i_{sdr} \tag{2.20c}$$

Another PI controller is employed over the amplitude of AC terminal voltage at point of common coupling to regulate the terminal voltage. The AC terminal voltage is filtered through low pass filter to obtain DC component. The output of this PI controller is shown in the equation (2.21).

$$i_{acq}(n) = i_{acq}(n-1) + k_p' \{V_{ae} - V_{ae}(n-1)\} + k_i' V_{ae}(n) \tag{2.21}$$

where, $V_{ae(n)} = V_{tmr} - V_{tm(n)}$ denotes the error between sensed AC voltage and reference AC voltage at point of common coupling. k_p' and k_i' are proportional and integral gains of AC voltage PI controller. The amplitude of reactive load current I_{sq} is calculated from equation (2.22).

$$I_{sq} = \frac{2}{3} \times \frac{\overline{q}}{V_{tm}} \tag{2.22}$$

The reactive power components of the source current are calculated as shown in equation (2.23), (2.24a), (2.24b) and (2.24c).

$$i_{sqr} = i_{acq} + I_{sq} \tag{2.23}$$

$$i_{sqar} = w_a \times i_{sqr} \tag{2.24a}$$

$$i_{sqbr} = w_b \times i_{sqr} \quad (2.24b)$$

$$i_{sqcr} = w_c \times i_{sqr} \quad (2.24c)$$

Hence in voltage regulation mode of operation the total reference currents for all the three phases are obtained by respectively adding the amplitude of active and reactive component of the load current as are shown in equation (2.25a), (2.25b) and (2.25c).

$$I_{sar} = i_{sdar} + i_{sqar} \quad (2.25a)$$

$$I_{sbr} = i_{sdbr} + i_{sqbr} \quad (2.25b)$$

$$I_{scr} = i_{sdcr} + i_{sqcr} \quad (2.25c)$$

The desired reference currents can be generated depending on mode of operation i.e. power factor improvement or voltage regulation. The three-phase reference currents so, calculated are compared with the sensed source currents and fed through hysteresis current controller to generate switching signals for D-STATCOM.

2.6.1. MATLAB based model and Simulation results

A model of distribution static compensator and its controller is developed in MATLAB environment using SIMULINK and Sim Power System (SPS) toolboxes is shown in Fig. 2.15. The performance of distribution static compensator is evaluated in MATLAB environment using SIMULINK and SPS toolboxes. The DC voltage of D-STATCOM is selected 200V for the source voltage of 110V. For self supporting DC bus voltage of D-STATCOM, a capacitor of 1640µF is used. The VSC is connected through 3.4mH inductor to the network. A non linear load is a three phase diode rectifier with resistance of 35Ω and inductor 100mH in series. The simulation results are taken for both power factor correction (PFC) and zero voltage regulation (ZVR) for the same load conditions. The results are obtained for two different cases.

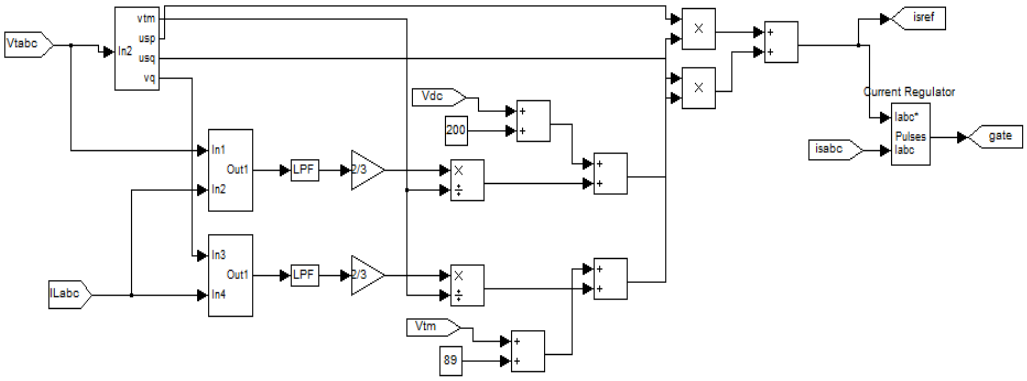

Fig. 2.15. MATLAB based model of PBT

2.6.1.1. Result for power factor improvement

The performance of D-STATCOM has been analyzed under steady state and dynamic condition for power factor correction, harmonic reduction and load balancing. Fig. 2.16 show the plot of real power of load and Fig. 2.17 show the plot of reactive power of the load under steady state condition. The simulation result shows that DC link voltage reaches it steady state value at t=0.06 seconds and remains in steady state till t=0.3 seconds. In the non linear load, phase 'c' is removed from t=0.3seconds to t=0.4 seconds. At t = 0.3seconds, when load phase 'c' is removed there is rise in DC link voltage and it regain its steady state value within few cycles. At t=0.4 seconds when phse 'c' is added there is dip in DC link voltage and it regain its steady state value within few cycle. The source voltage ($v_{sa,}$ $v_{sb,}$ v_{sc}), source current ($i_{sa,}$ $i_{sb,}$ i_{sc}), compensator current ($i_{ca,}$ $i_{cb,}$ i_{cc}), load current ($i_{la,}$ $i_{lb,}$ i_{lc}), DC bus voltage (V_{dc}), PCC voltage (V_{tm}) are shown in Fig. 2.18. It is observed that the source currents are balanced, harmonic free and in phase with PCC voltage irrespective of balanced or unbalanced load conditions as the loads are compensated by D-STATCOM. The DC bus voltage is also regulated to its reference value. Fig. 2.19 shows the THD waveform of source current and Fig.2.20 shows THD waveform of load current. The THD of source current is 3.94% when load current THD is 28.16%.

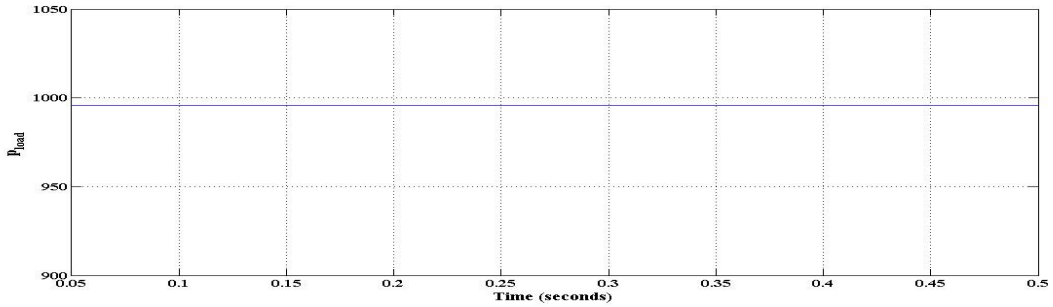

Fig. 2.16. Plot of real load power (p_{load}) under steady state condition

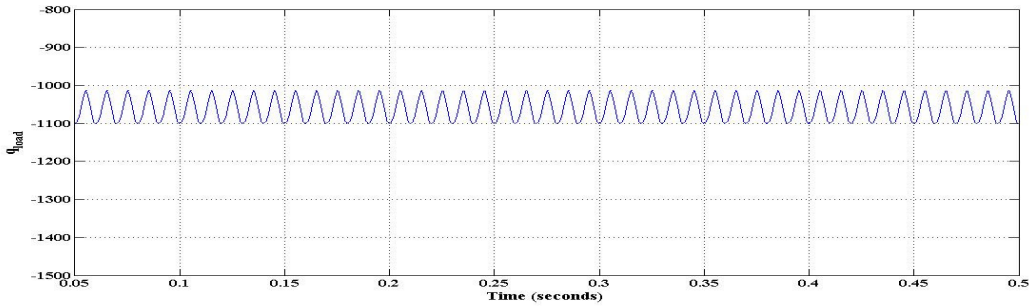

Fig. 2.17. Plot of reactive load power (q_{load}) under steady state condition

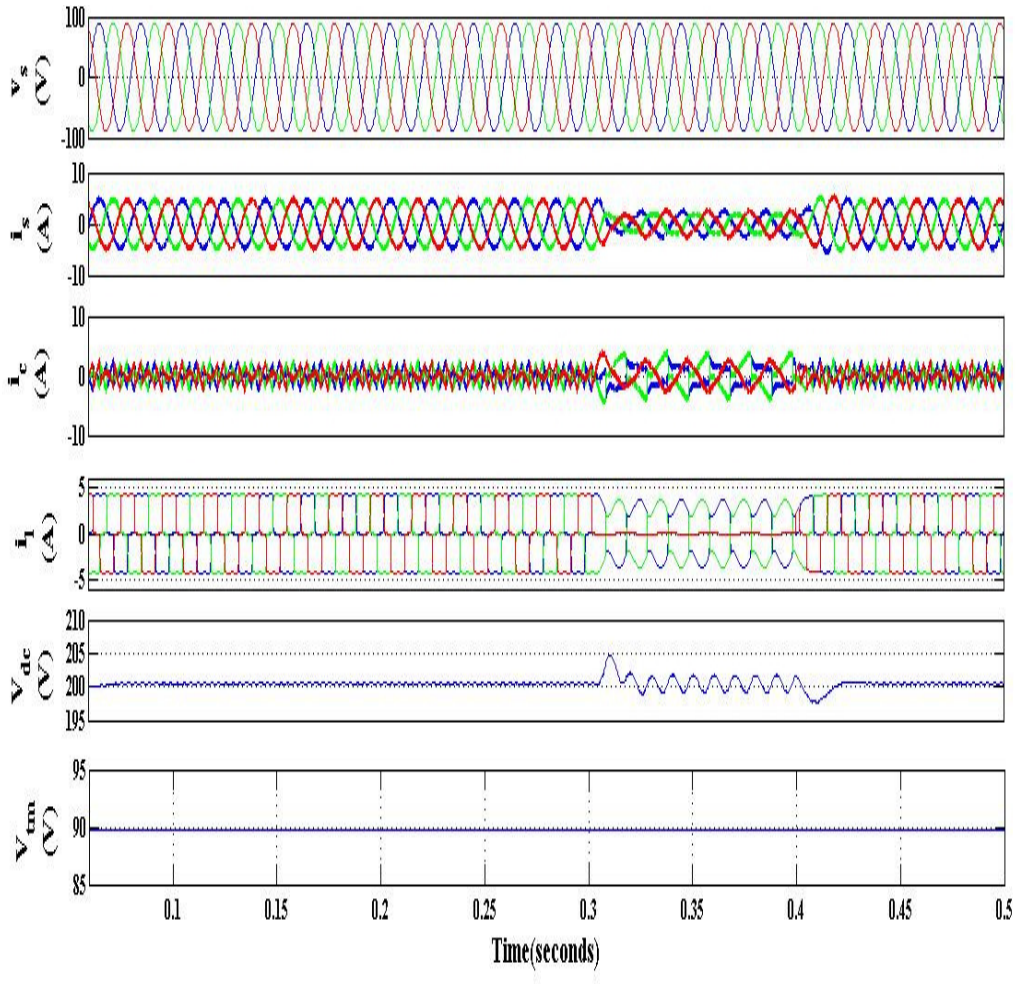

Fig.2.18. Waveform of source voltage (v_s), source current (i_s), compensator current (i_c), load current (i_l), dc voltage (V_{dc}), terminal voltage V_{tm}.under balanced/unbalanced condition (UPF mode)

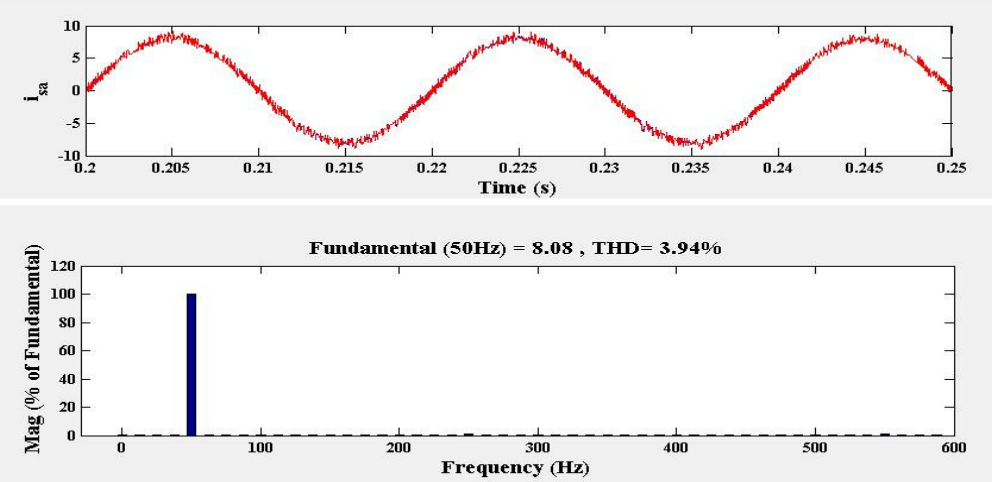

Fig. 2.19. Waveform and THD of source current (i_{sa})

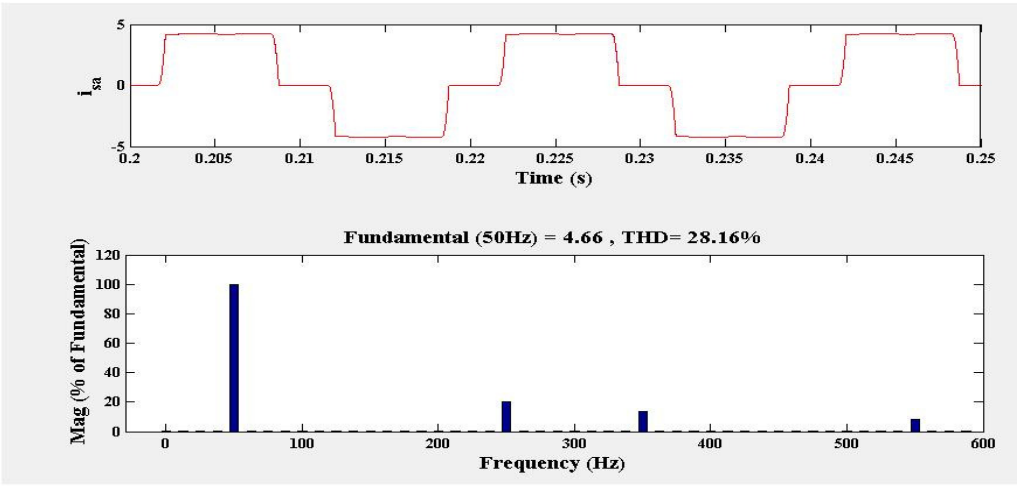

Fig. 2.20. Waveform and THD of load current (i_{la})

2.6.1.2. Result for Voltage Regulation

The performance of D-STATCOM in Voltage regulation mode is evaluated for the same load conditions as in PFC mode. The results in Fig. 2.21 shows waveform of source voltage (v_s), source current (i_s), compensator current (i_c), load current (i_l), dc voltage (V_{dc}), terminal voltage V_{tm} under balanced/unbalanced condition. The system remains in steady state condition till t=0.2 seconds, after which at t= 0.2 seconds phase 'c' is removed and at t=0.3 seconds phase 'b' is removed. It is observed that the PCC voltage regulates to reference value under both balanced and unbalanced conditions. DC voltage slight rises as phase 'b' and 'c' and maintained to its reference voltage by the controller actions. Similarly, when phase 'b' and 'c' are again added to the system at t= 0.3 seconds and t= 0.4 seconds, the DC voltage is again maintained at reference value. It is seen that non linear load is compensated by D-STATCOM and make the source currents harmonic free and balanced when the non linear load is unbalanced. Fig. 2.22 and Fig. 2.23 shows THD of source current and load current respectively. The THD of source current is 4.24% when the THD of load current is 28.16%.

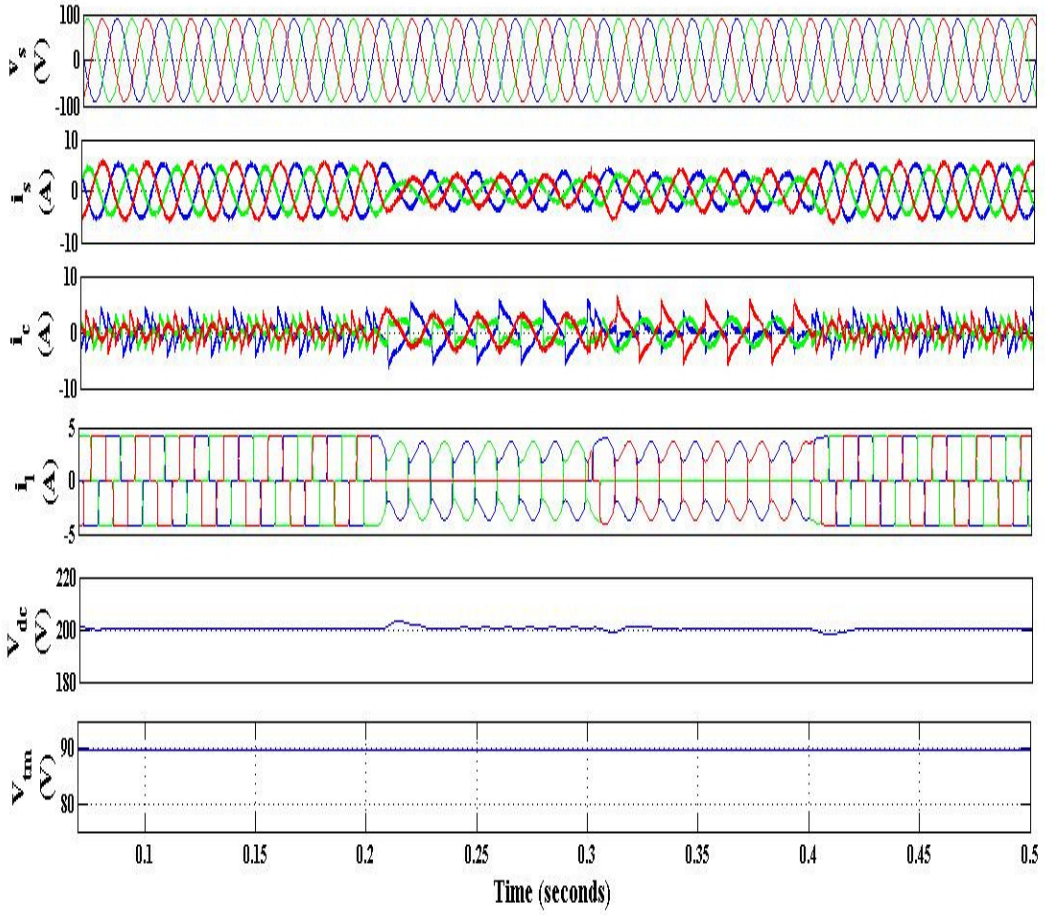

Fig. 2.21. Waveform of source voltage (v_s), source current (i_s), compensator current (i_c), load current (i_l), dc voltage (V_{dc}), terminal voltage V_{tm}.under balanced/unbalanced condition (voltage regulation mode)

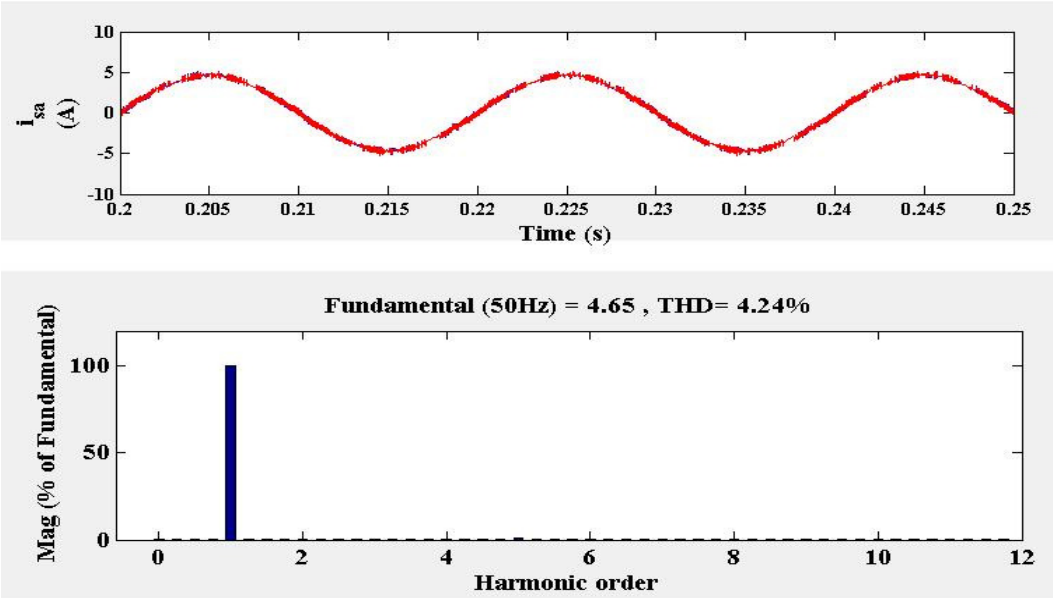

Fig. 2.22. Waveform and THD of source current (i_{sa})

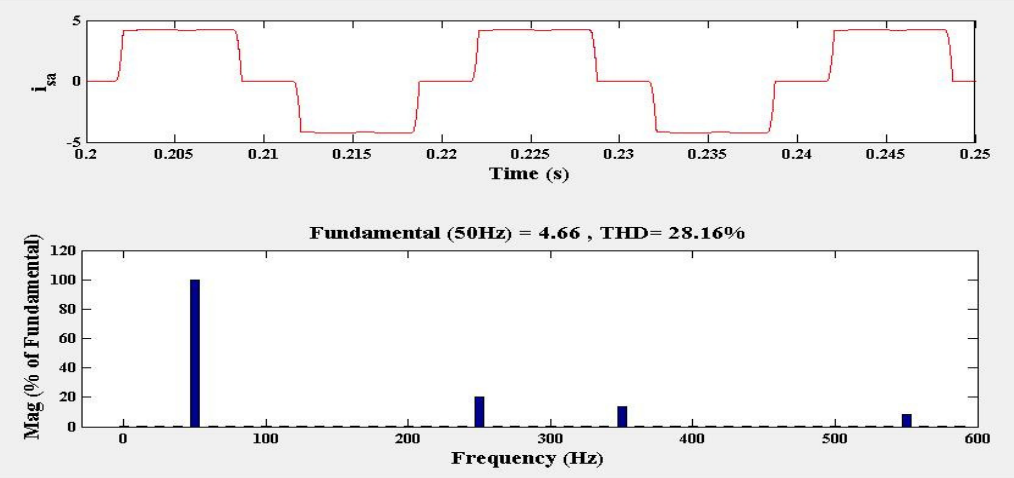

Fig. 2.23. Waveform and THD of load current i_{la}

2.7. Hardware Results

The system details for hardware implementation are mentioned in the Appendix. The same parameters chosen for simulation are considered for hardware implementation. A prototype of D-STATCOM is developed using 'Semikron' three leg VSC with six IGBTs. Five current sensors (LEM LA25) and four voltage sensors (LEM LV 25) are used for sensing various current and voltage signals. The proposed control model is implemented using dSPACE DS1104 processor. The test results recorded using fluke 43B power analyzer. The performance of D-STATCOM is tested for different non-linear load conditions in PFC mode.

Fig. 2.24 shows the waveform of source current (i_{sa}), load current (i_{la}) and compensator current (i_{ca}) with DC link voltage (V_{dc}) under steady state condition. Fig. 2.25 shows the dynamic condition of D-STATCOM in which load from phase 'c' is removed. The load current in phase 'c' becomes zero. This results in sudden increase in DC link voltage which settle down to its reference value very quickly by controllers action. During phase removal D-STATCOM supplies increased compensator current to make supply current in phase 'c' sinusoidal and thus the source current reduces slightly and remain balanced. In Fig. 2.26 phase 'c' is added to remove unbalancing thus the load current (i_{lc}) increases. This results in sudden dip in the DC link voltage which settle down to its reference value very quickly. This causes reduction in compensator current and increase in source current. The source current remains in balanced condition. The non-linear loads current are compensated by D-STATCOM to make the source current harmonic free and balanced even though the non-linear load is unbalanced.

Fig. 2.27 shows the source voltage and source current waveform which are sinusoidal. Fig. 2.28 shows the THD of source current in phase 'a' which is 4.7%. The THD of load current in phase 'a' is 23.9% which is shown in Fig. 2.29. The THD of PCC voltage is shown in Fig. 2.30 which is 3.1%. These results show the effective performance of control algorithm.

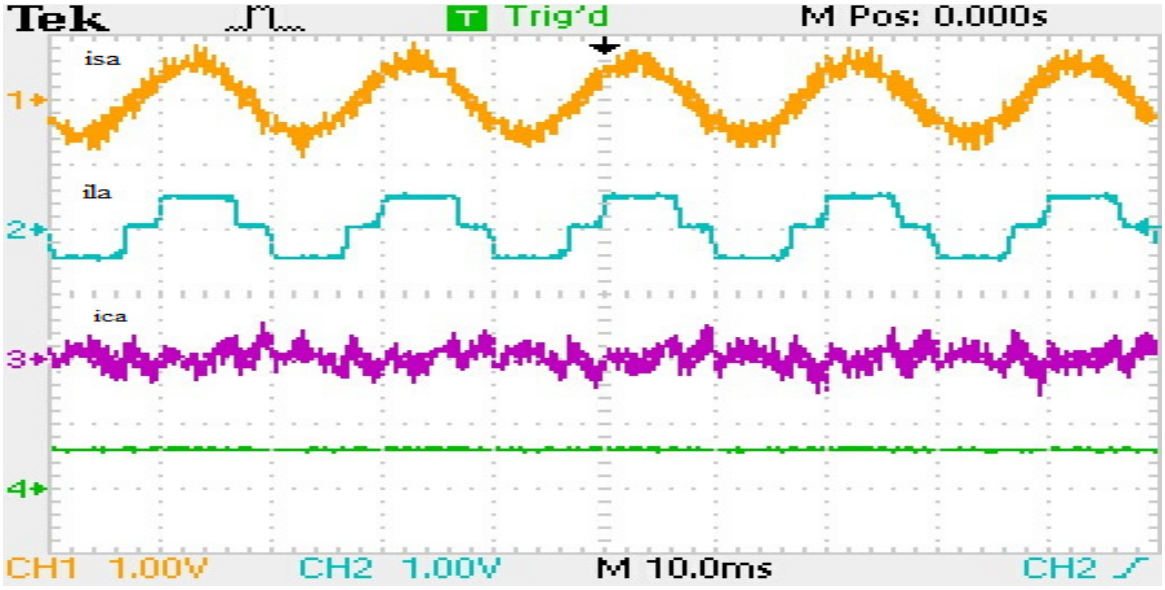

Fig. 2.24. Steady state waveform of source current (i_{sa}), load current (i_{la}), compensator current (i_{ca}) and DC voltage (V_{dc})

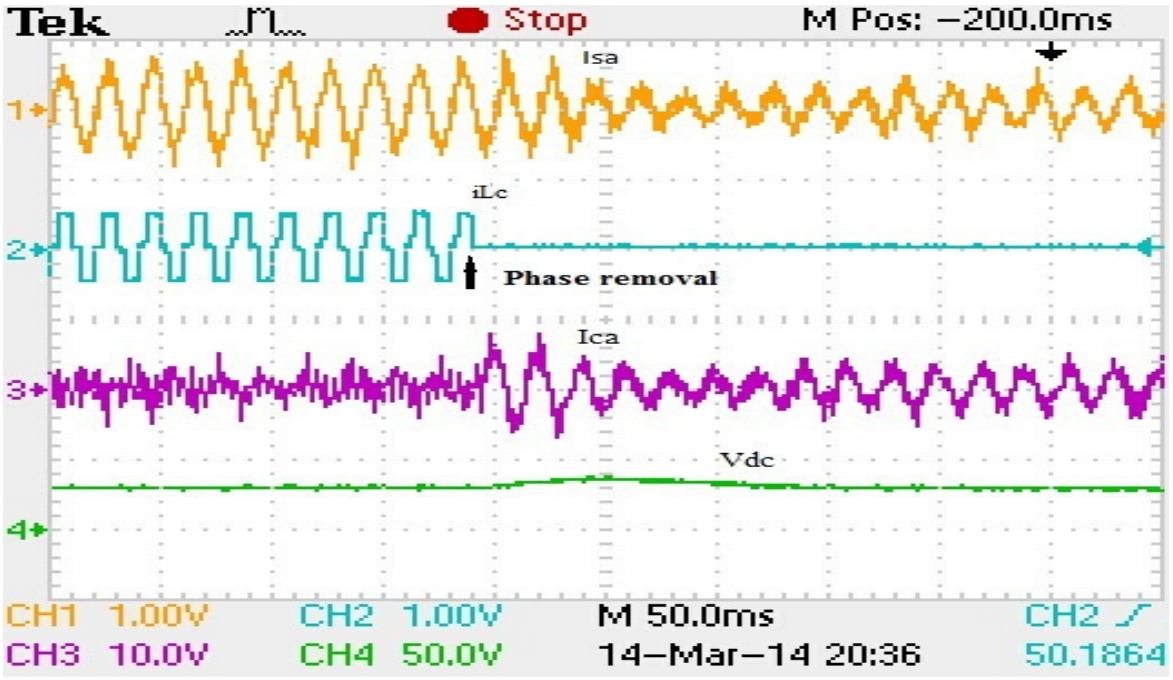

Fig. 2.25. Waveform of source current (i_{sa}), load current (i_{lc}), compensator current (i_{ca}) and DC link voltage (V_{dc}) when load is removed in phase 'c'

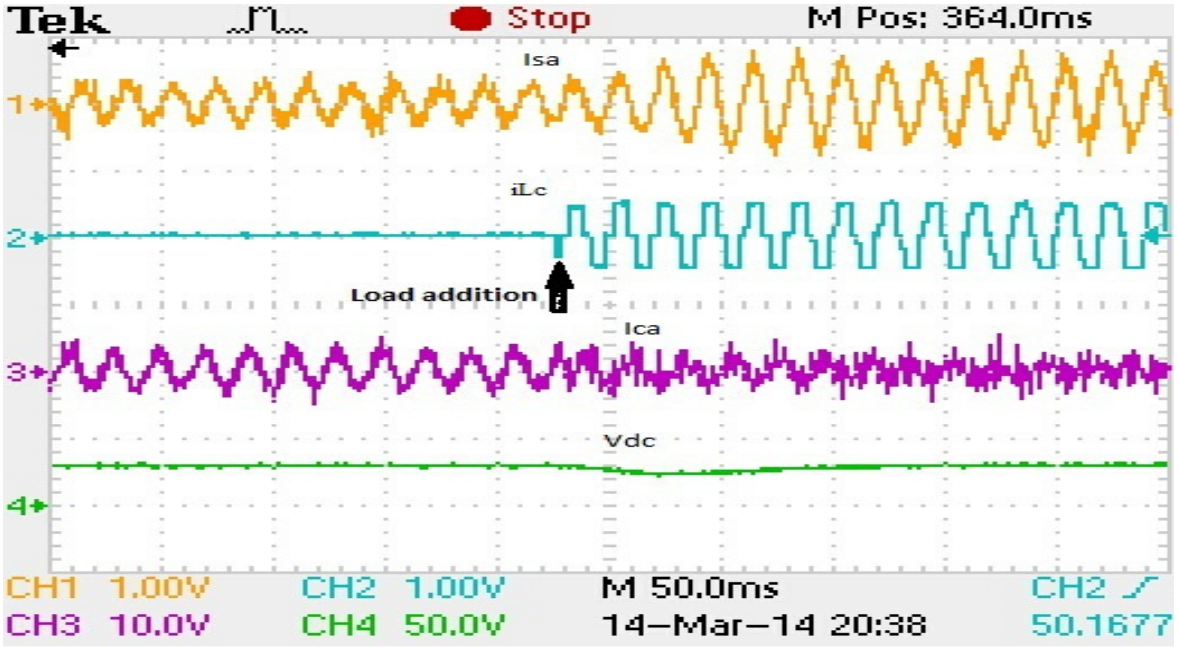

Fig. 2.26. Waveform of source current (i_{sa}), load current (i_{lc}), compensator current (i_{ca}), DC link voltage (V_{dc}) when load in phase 'c' added

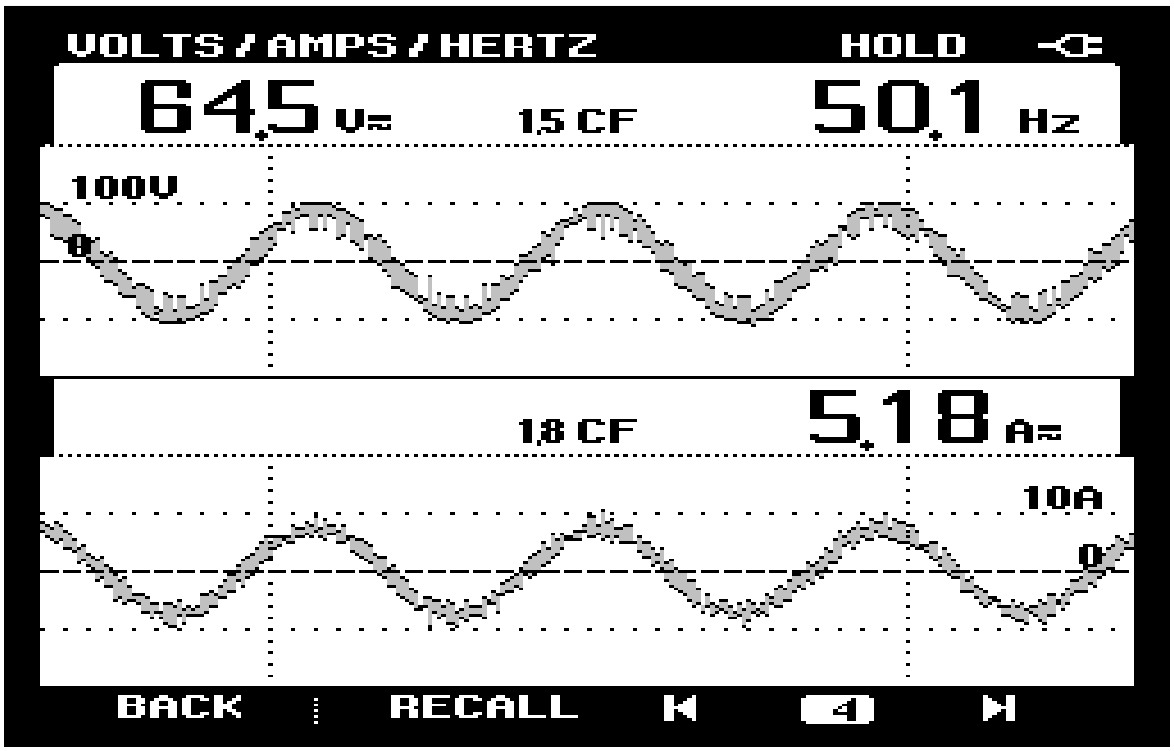

Fig. 2.27. Waveform of source current (i_{sa}) and source voltage (v_{sa})

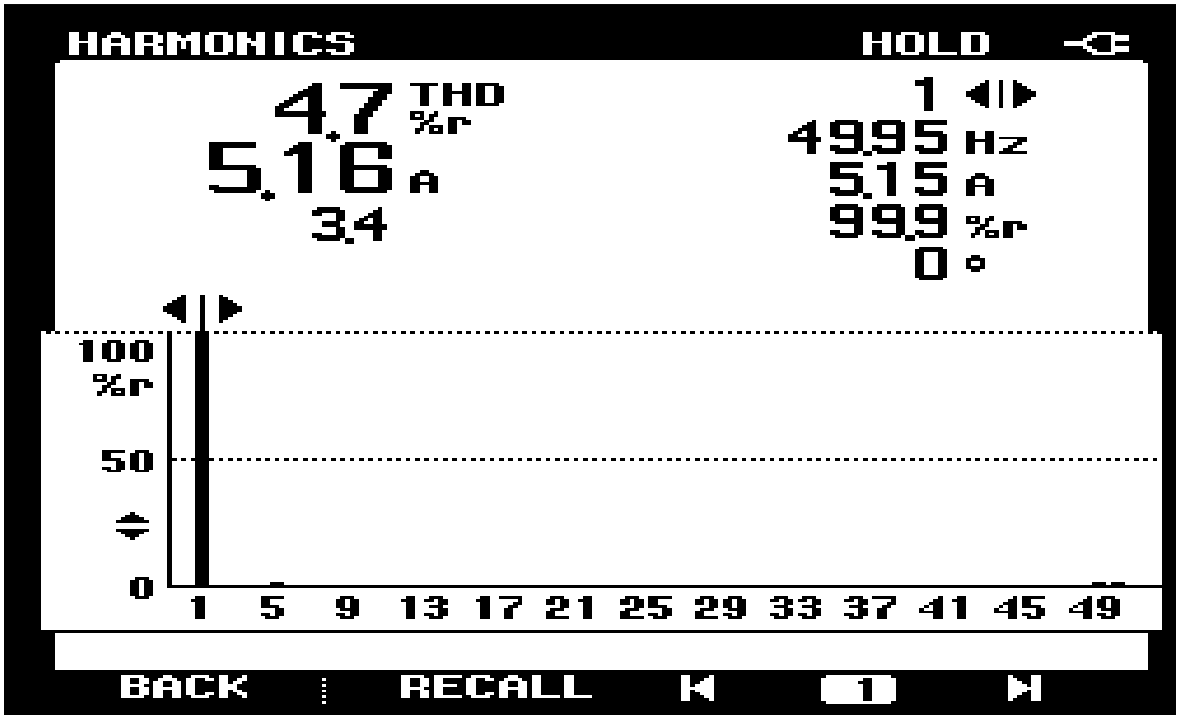

Fig. 2.28. THD of source current (i_{sa})

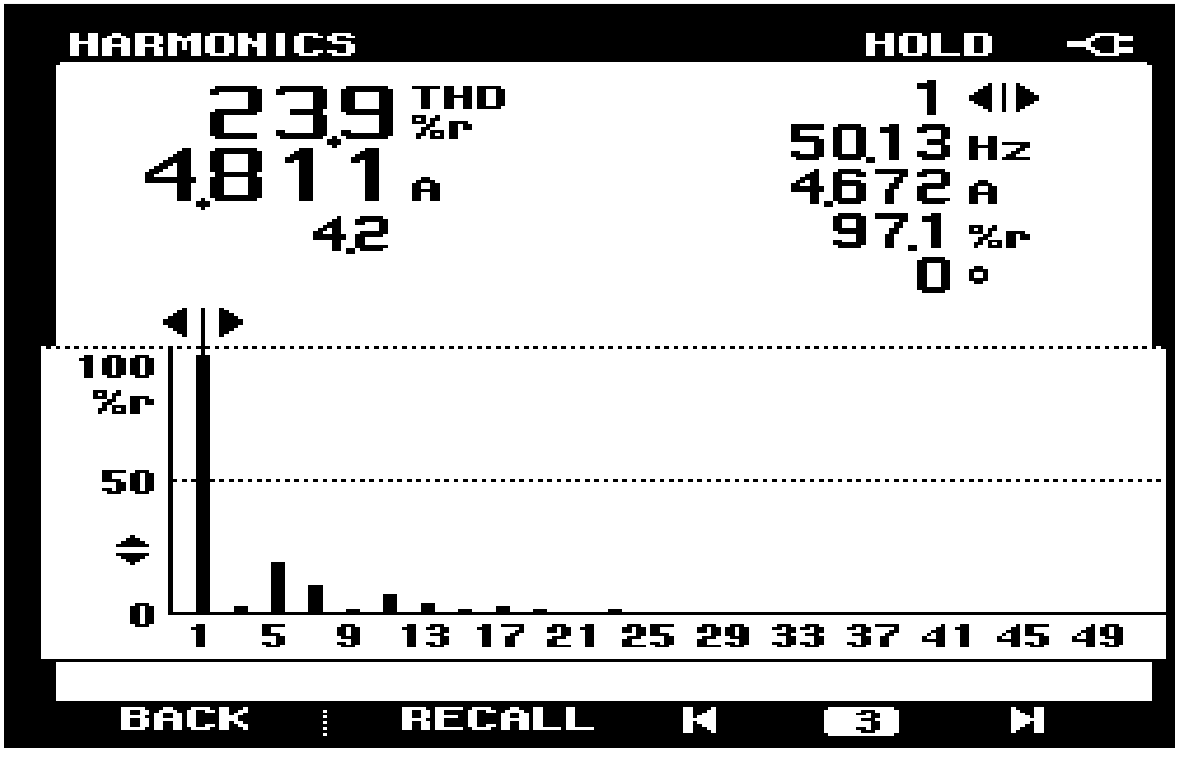

Fig. 2.29. THD of load current (i_{la})

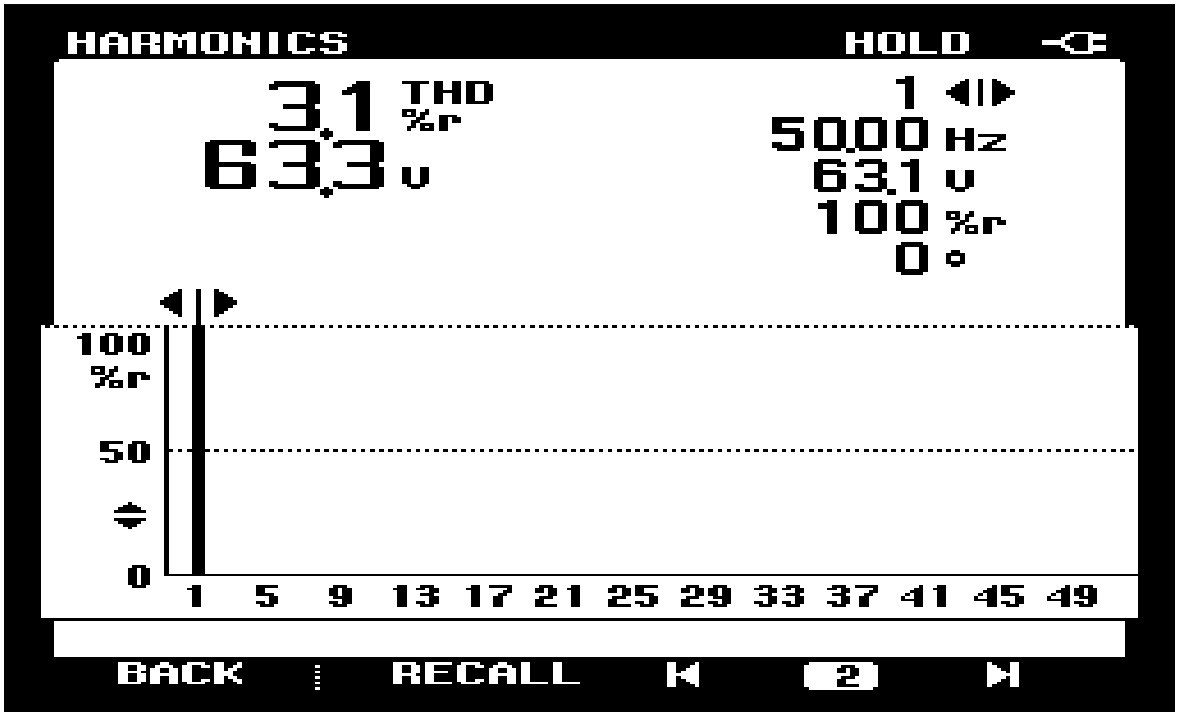

Fig. 2.30. THD of source voltage (v_{sa})

2.8. Conclusion

The results are illustrated for non-linear load in both steady state and dynamic load conditions. MATLAB model is implemented in Sim Power System and three phase reference supply currents are evaluated using power balance theory. Prototype model is developed using the same simulation parameters. Simulation as well as hardware implemented results show THD of less than 5% in the supply current with non linear load currents. Extensive simulation and hardware result have been shown which prove that D-STATCOM can be controlled using power balance control algorithm for mitigating various power quality problems.

Chapter3

Fuzzy logic controller

3.1. General

Conventional controllers are used in various industrial process applications. These include PI or PD or PID controllers with fixed feedback gain. This needs heuristic approach i.e. hit and trial method to get the desired results thus controller may or may not give satisfactory results in all cases of load perturbation. Such controllers have few drawbacks they are not flexible or adaptable to changes in system parameters and to the presence of disturbance and noise in the system, hence their performance sometimes deviates producing unsatisfactory results. Conventional controller parameter uses linear mathematical model for system evaluation and has computational complexity. This drawback can be alleviated by replacing the conventional controllers by an intelligent controller that can learn and control the system intelligently [45].

3.2. Fuzzy logic theory

Fuzzy logic controller (FLC) is a controller which does not require mathematical modeling. Fuzzy logic is synonymous to the theory of fuzzy set. FLC uses linguistic approach for formulation of fuzzy rules which means it uses words for defining the variables values rather than numbers. These are easier to understand. The trend of using Adaptive intelligence is growing nowadays. Fuzzy logic, neural network, genetic algorithm, particle swarm optimization techniques etc categorize into soft computing techniques. FLC can also be used alone or in combination with other soft computing techniques. In fuzzy logic, expert's knowledge and experience is used for deciding fuzzy membership function and making fuzzy rules. The input and output of non-linear processes can be well defined through qualitative set of "if-then" fuzzy rules.

3.3. Design of fuzzy logic controller

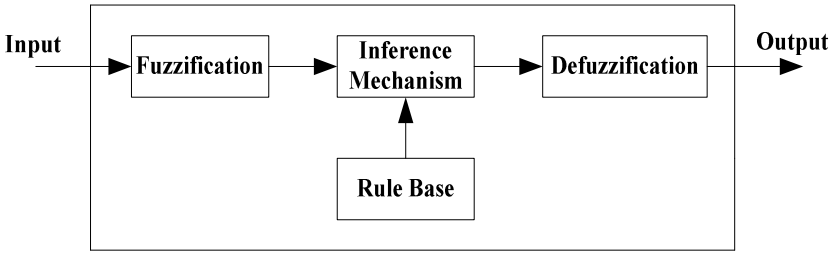

Fig. 3.1. Block diagram of Fuzzy Logic Controller

Fig.3.1 shows the basic aspects of fuzzy logic controller. An input is taken in specific form that can be passed through different blocks of fuzzy logic controller to get the specific form of output. The different stages in fuzzy logic controller have been described below:

3.3.1. Fuzzification

An input data is passed through fuzzification process to form a fuzzy set. It is a process that converts the input quantity into fuzzy set that can be inferred easily through inference mechanism. Fuzzification is done using continuous universe of discourse. The input signals are crisp signals which are assigned the membership functions. These membership functions are assigned some range of values under which input signal falls. There are different types of membership functions can be used to define input variable like triangular, trapezoidal, guassian, sigmoid etc [46]. For simulation purpose triangular function is found to be more suitable in evaluating results appropriately.

3.3.2. Inference Mechanism

The input variables used are the error and the change in error in DC link voltage to determine the rules to be applied. After determining the rules, the control action is ascertained from the value of the membership function. This process is called premise quantification. Based on database rules are formed that are presented in the rule base to obtain appropriate control action.

3.3.3. Design of Fuzzy Logic Rules

Designing of the fuzzy rules is very important for the proper operation of the controller. The formulation of fuzzy rules is based on the step response of the closed loop system

whose shape is shown in the Fig 3.2 and analysis of the system behavior. There are two input variables for fuzzy logic controller and one output variable. One input variable is the error (er) between the actual voltage across the capacitor and reference voltage which is taken as 200V. The second input variable is the change in error (Δer). The output variable of FLC represents the loss component of the inverter. The time response has been divided into different regions depending on the sign of the error (er) and change of error (Δer).

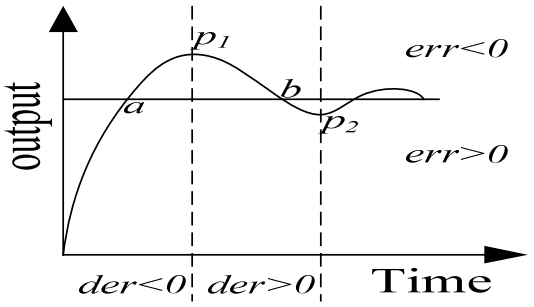

Fig. 3.2. Closed Loop Response of Step Input

These are four regions

Region 1: for er >0 and cer<0

Region 2: for er<0 and cer<0

Region 3: for er<0 and cer>0

Region 4: for er>0 and cer>0

There are crossing points (a & b):

a: change of error from positive to negative value

b: change of error from negative to positive value

There are two peak valleys (p1 & p2):

p_1: cer = 0 and er <0

p_2: cer=0 and er>0

3.3.4. Defuzzification Mechanism

Defuzzification is the process in which consider the rules and the membership functions and their combined effect is converted into crisp form and output is produced in numerical form. Here “center of gravity” is used for defuzzification process.

3.4. MATLAB based model and Simulation Results

Fig. 3.3 shows the block diagram of the system where the conventional PI controller has been replaced by fuzzy logic controller. The output of FLC is loss component (i_{loss}) of the converter which is processed further.

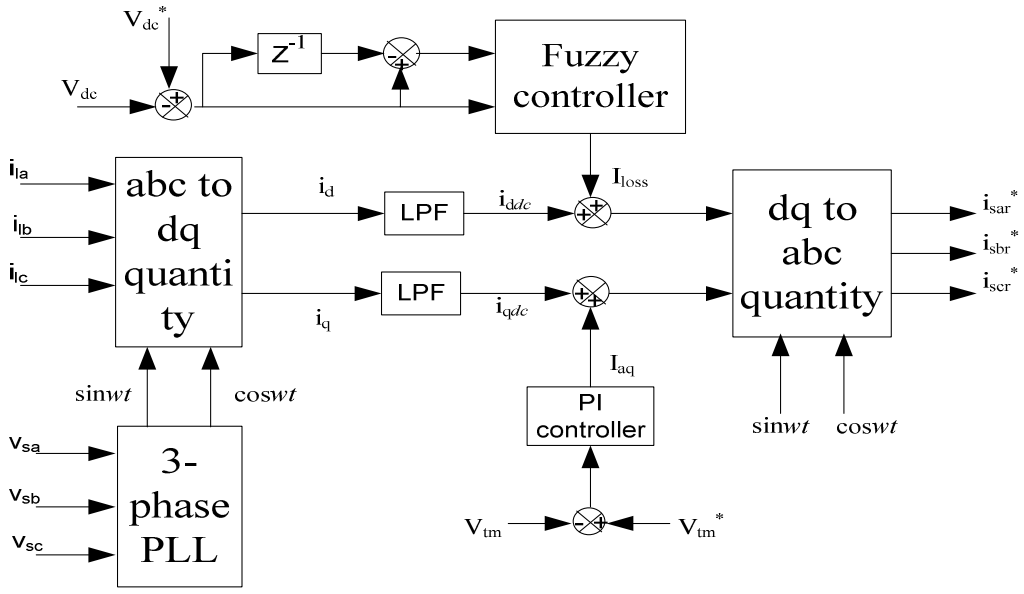

Fig. 3.3. Block diagram of Fuzzy Logic Control Scheme

3.4.1. FLC based on 49 rules

The fuzzy rules are partitioned into seven subsets that are NL, NM, NS, Z, PS, PM, PL for both the error (er) and change of error (Δer) input variables are shown in the Table 3.1.

These rules are formed in MATLAB environment using fuzzy logic controller toolbox. Fig.3.4 (a), (b) and (c) shows the triangular membership function for defining the rules for input variables and output variable.

Table 3.1. Fuzzy logic controller rules for seven rule base (49 rules)

Δer / er	NL	NM	NS	Z	PS	PM	PL
NL	*NL*	*NL*	*NL*	*NL*	*NM*	*NS*	*Z*

NM	*NL*	*NL*	*NL*	*NM*	*NS*	*Z*	*PS*
NS	*NL*	*NL*	*NM*	*NS*	*Z*	*PS*	*PM*
Z	*NL*	*NM*	*NS*	*Z*	*PS*	*PM*	*PL*
PS	*NM*	*NS*	*Z*	*PS*	*PM*	*PL*	*PL*
PM	*NS*	*Z*	*PS*	*PM*	*PL*	*PL*	*PL*
PL	*Z*	*PS*	*PM*	*PL*	*PL*	*PL*	*PL*

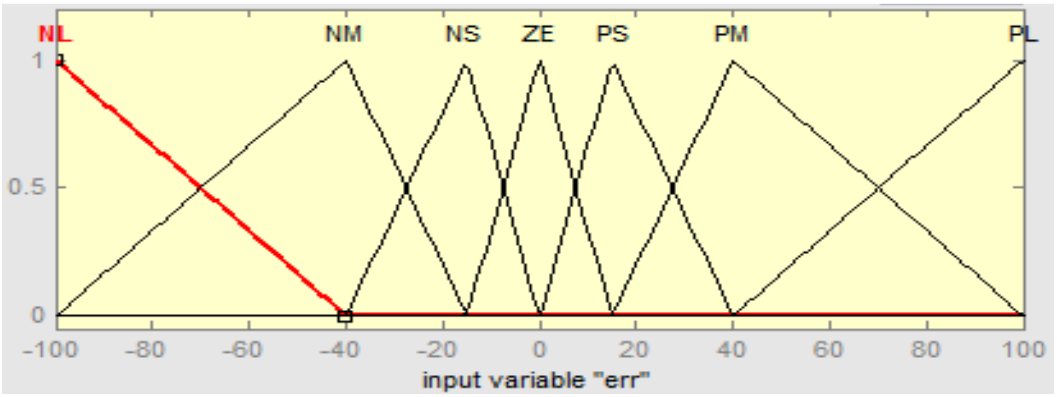

(a)

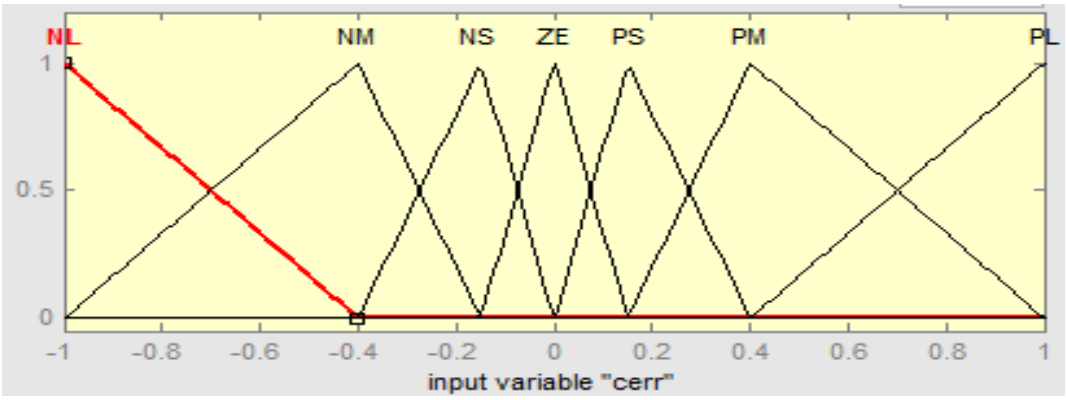

(b)

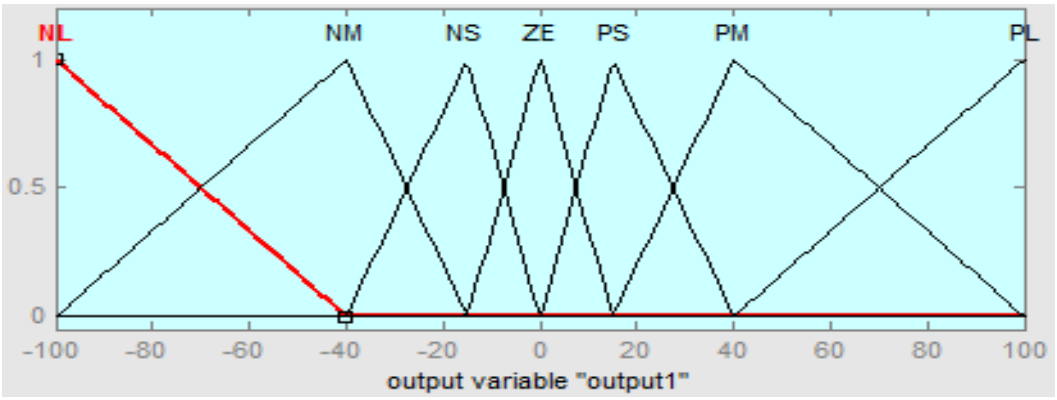

(c)

Fig. 3.4. Seven Rulebase for (a) input (er) (b) input (Δer) (c) output (i_{loss})

3.4.1.1 Results for Power Factor Improvement under Steady state and Dynamic Conditions

Fig. 3.5 shows the waveforms of source voltage, source current, compensator current, load current, dc link voltage and voltage at PCC. At t= 0.2 seconds, the load is changed by adding 40Ω resistor which changes the current from 4A to 7.4.A. It is observed from the plot that there is a very slight dip in DC link voltage and it regains its reference value in less than half cycle. At t=0.25 seconds, 40Ω load is removed and from t=0.26 seconds to t=0.3 seconds, 30 Ω load resistor is added which changes the load current from 7.4A to 12 A. FLC controller regulates the DC link voltage and less than 1V DC link voltage dip occurs. DC voltage (V_{dc}) settles to its reference value of 200V and PCC voltage is maintained. Fig. 3.6 shows that source voltage and source current waveforms are in phase 'a' with each other. The THD waveform of source current is 2.37% is shown in Fig. 3.7. The DC link voltage plot is shown in Fig. 3.8. It is observed that DC link voltage settles to reference value in less than two cycles. The FLC controller regulates the DC link voltage even when the load changes.

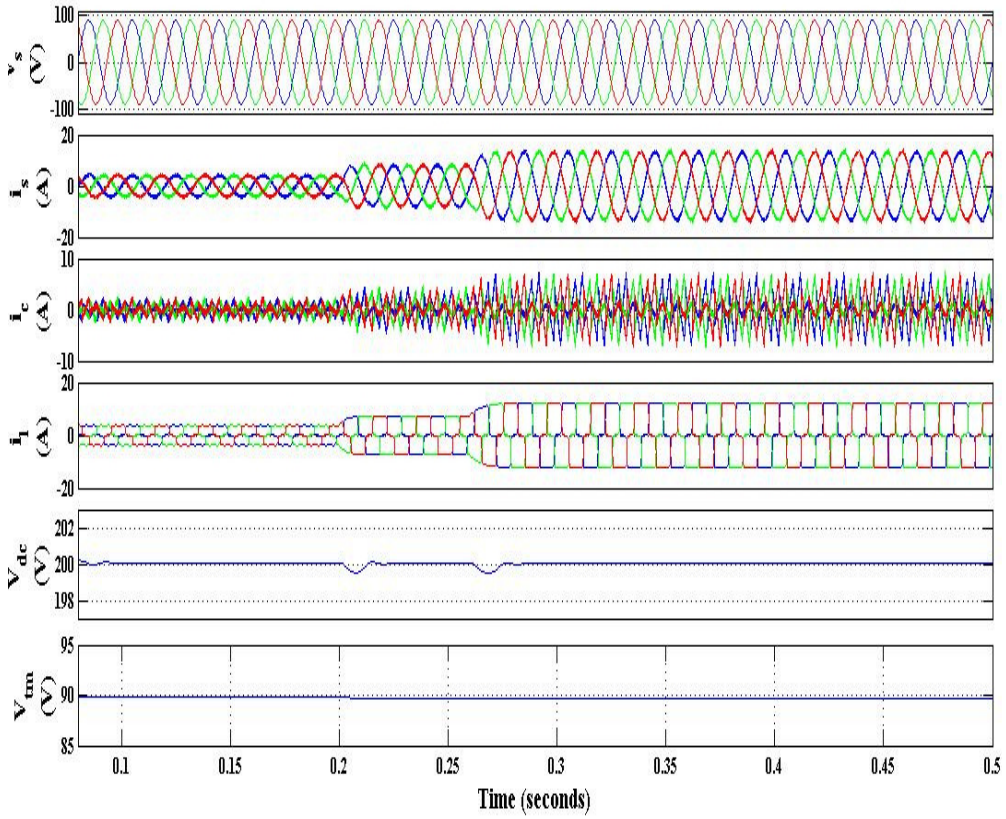

Fig. 3.5. Result showing source voltage (v_s), source current (i_s), compensator current (i_c), load current (i_l), DC link voltage (V_{dc}) and voltage at PCC (V_{tm}) under steady state / dynamic condition (UPF mode)

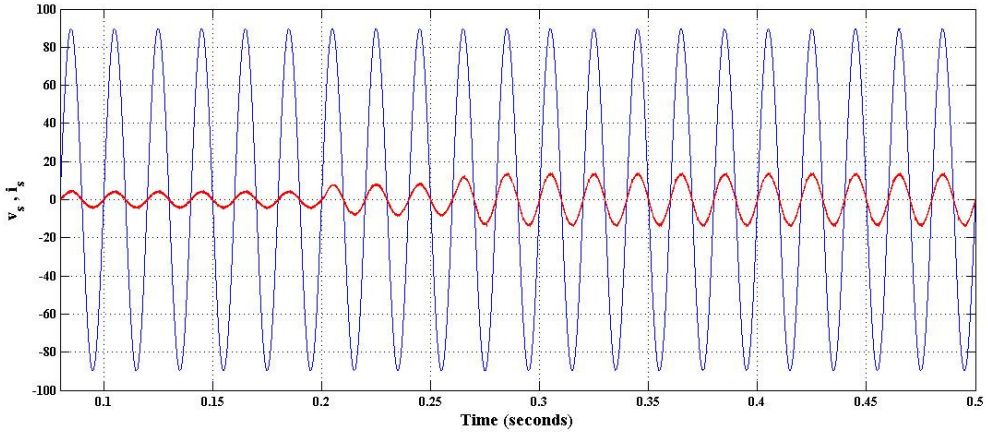

Fig. 3.6. Plot of source voltage (v_{sa}) and source current (i_{sa})

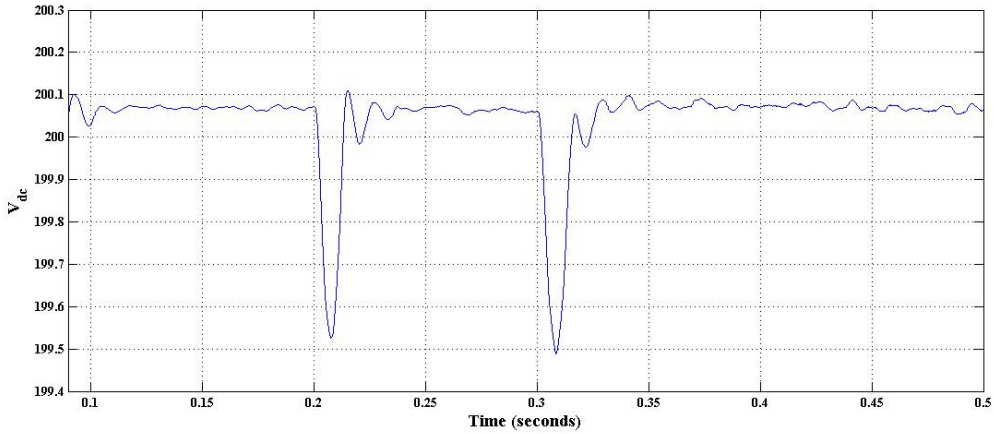

Fig. 3.7. DC link voltage (V_{dc}) variation with time under dynamic load changes

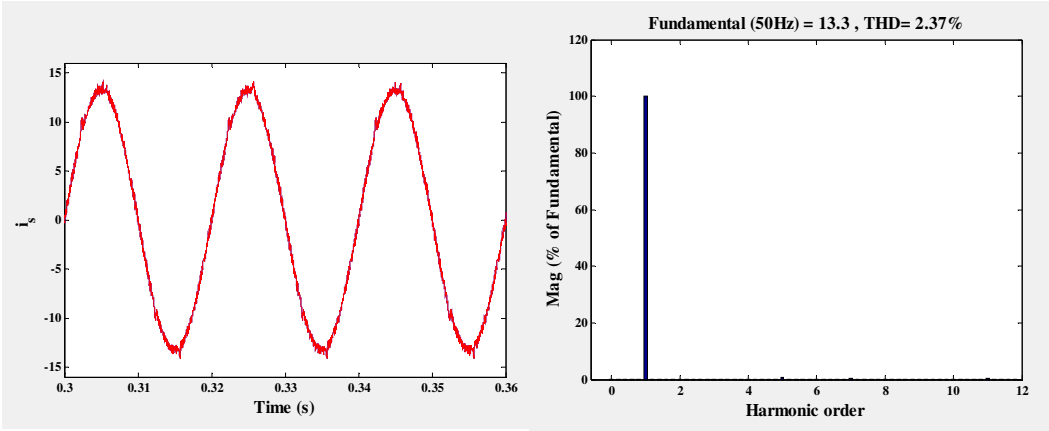

Fig. 3.8. Waveform and THD of source current (i_{sa})

3.4.1.2. Results for Voltage Regulation under steady state / dynamic conditions.

Fig. 3.9 shows the source voltage, source current, compensator current, load current, DC link voltage and voltage at PCC. The load conditions are taken to be same as for power factor correction. It is observed that DC link voltage is maintained to its reference value even when load is changed at t= 0.2 seconds and at t = 0.3seconds for voltage regulation. Thus, the source current becomes sinusoidal and has a THD content of 2.8% is shown in the Fig. 3.10.

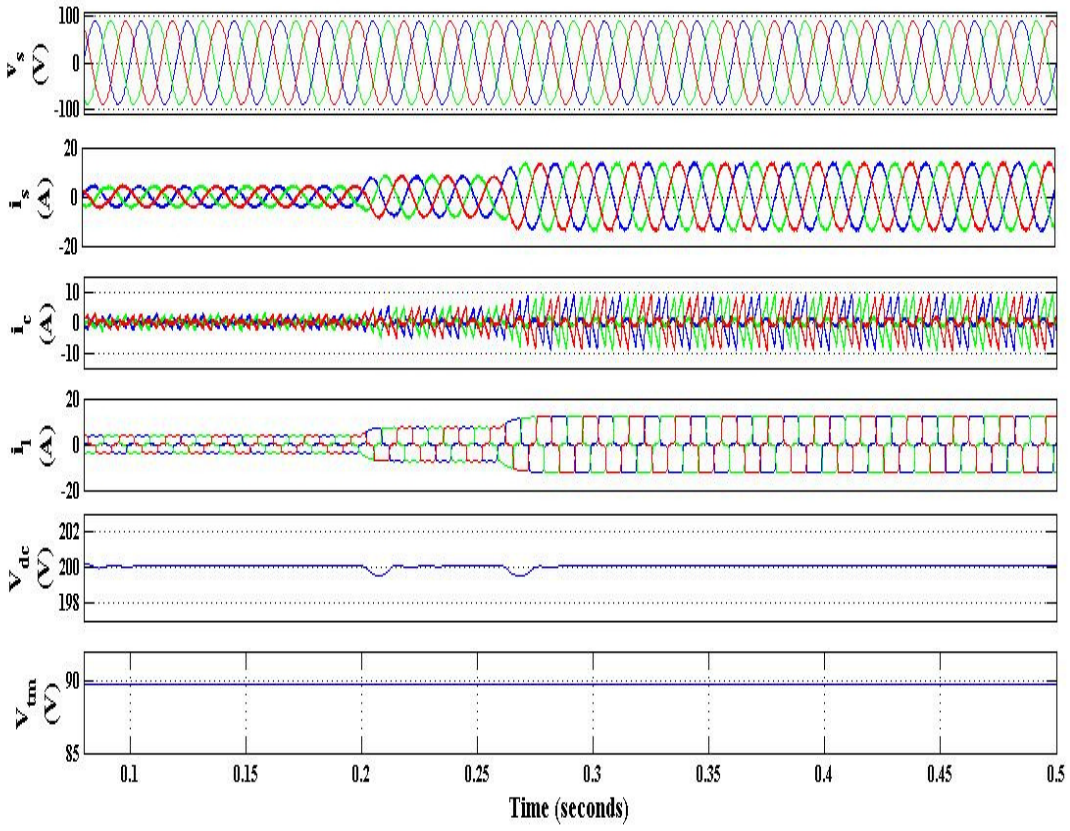

Fig. 3.9. Results showing source voltage (v_s), source current (i_s), compensator current (i_c), load current (i_l), DC link voltage (V_{dc}) and voltage at PCC (V_{tm}) under steady state / dynamic condition (voltage regulation)

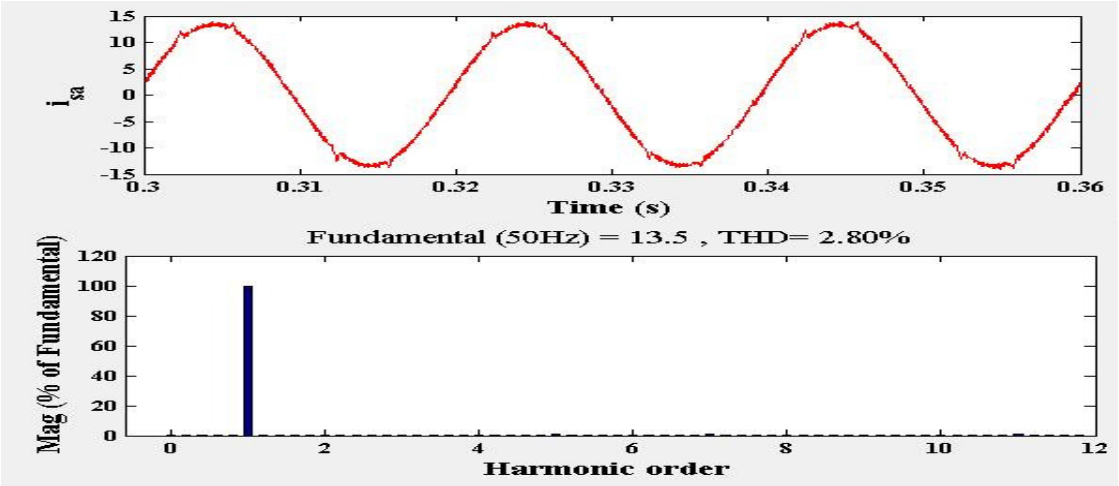

Fig. 3.10. Waveform and THD of source current (i_{sa})

3.4.2. FLC based on 25 rules

The fuzzy rules are partitioned into five subsets that are NM, NS, Z, PS, PM for both the error (er) and change of error (Δer) input variables are shown in the Table 3.2. Fig 3.11 (a), (b) and (c) shows the membership function for input and output variables.

Table 3.2. Fuzzy logic controller rules for five rule base (25 rules)

Δer / er	NM	NS	Z	PS	PM
NM	*NM*	*NM*	*NM*	*NS*	*Z*
NS	*NM*	*NS*	*NS*	*Z*	*PS*
Z	*NM*	*NS*	*Z*	*PS*	*PM*
PS	*NS*	*Z*	*PS*	*PM*	*PM*
PM	*Z*	*PS*	*PM*	*PM*	*PM*

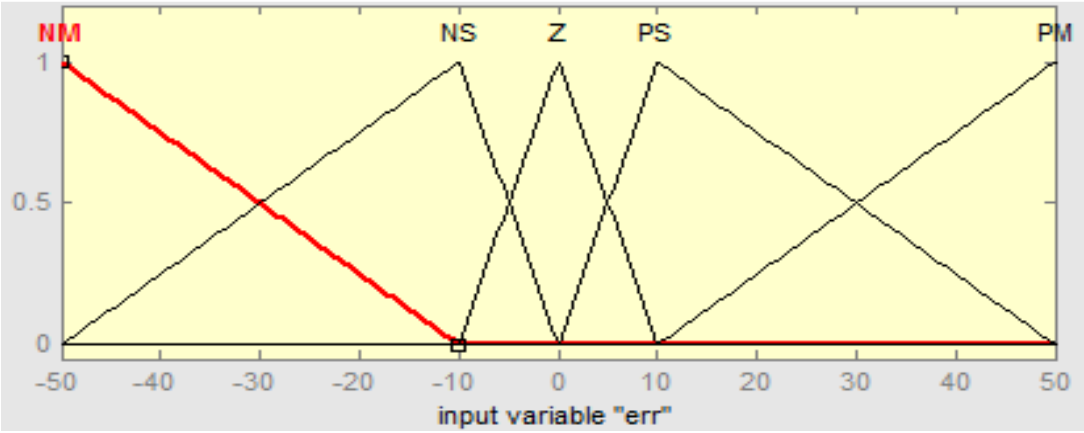

(a)

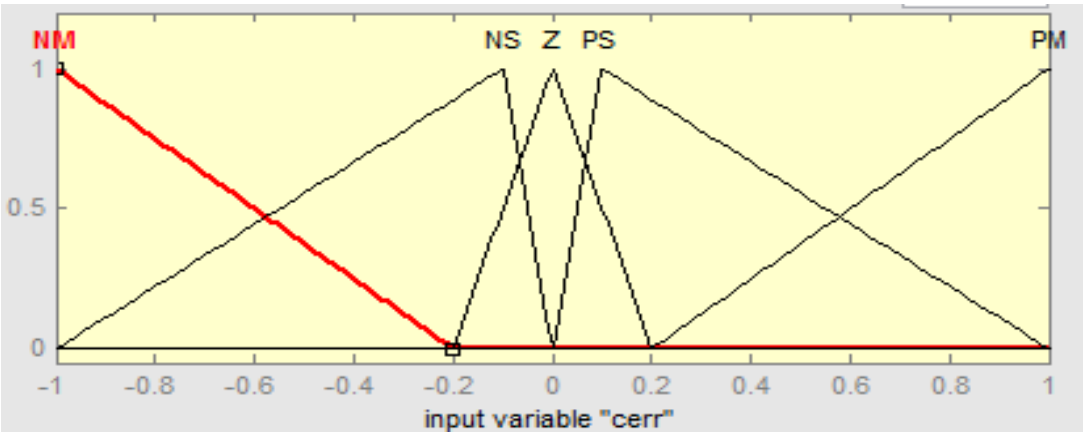

(b)

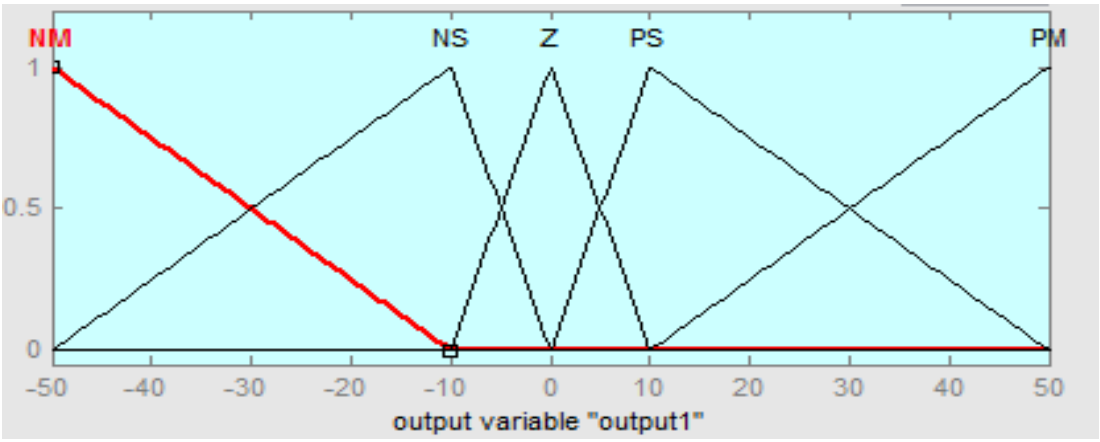

(c)

Fig. 3.11. FLC based on five rules (a) Input (er) (b) Input (Δer) (c) Output variables

3.4.2.1. Results for Power Factor improvement under steady state/ dynamic load conditions

Fig. 3.12 shows the waveforms of source voltage, source current, compensator current, load current, DC link voltage and voltage at PCC. For voltage regulation, another PI controller is used at point of common coupling. The voltage at PCC is sensed using sensor and compared with the reference PCC voltage. The error is passed through FLC controller. It is observed that the DC voltage is regulated to its reference value within 1-2 cycles when load change occurs. PCC voltage is also maintained to constant value of 89V. Fig. 3.13 shows the THD waveform of source current is 2.58% when the load current has THD of 28%.

Fig. 3.14 shows the DC link voltage plot. On comparing Fig. 3.7 and Fig. 3.14 it is observed that overshoot and undershoot voltage is less now than obtained with 49 rules fuzzy rules. It is also seen from the plot that when load current is increased from 4A to 7.4A at t=0.2seconds and from 7.4A to 12A at t=0.3seconds, there is a dip in DC link voltage due to load addition. However, the magnitude of dip is less than 0.5V with 25 rules than with 49 rules.

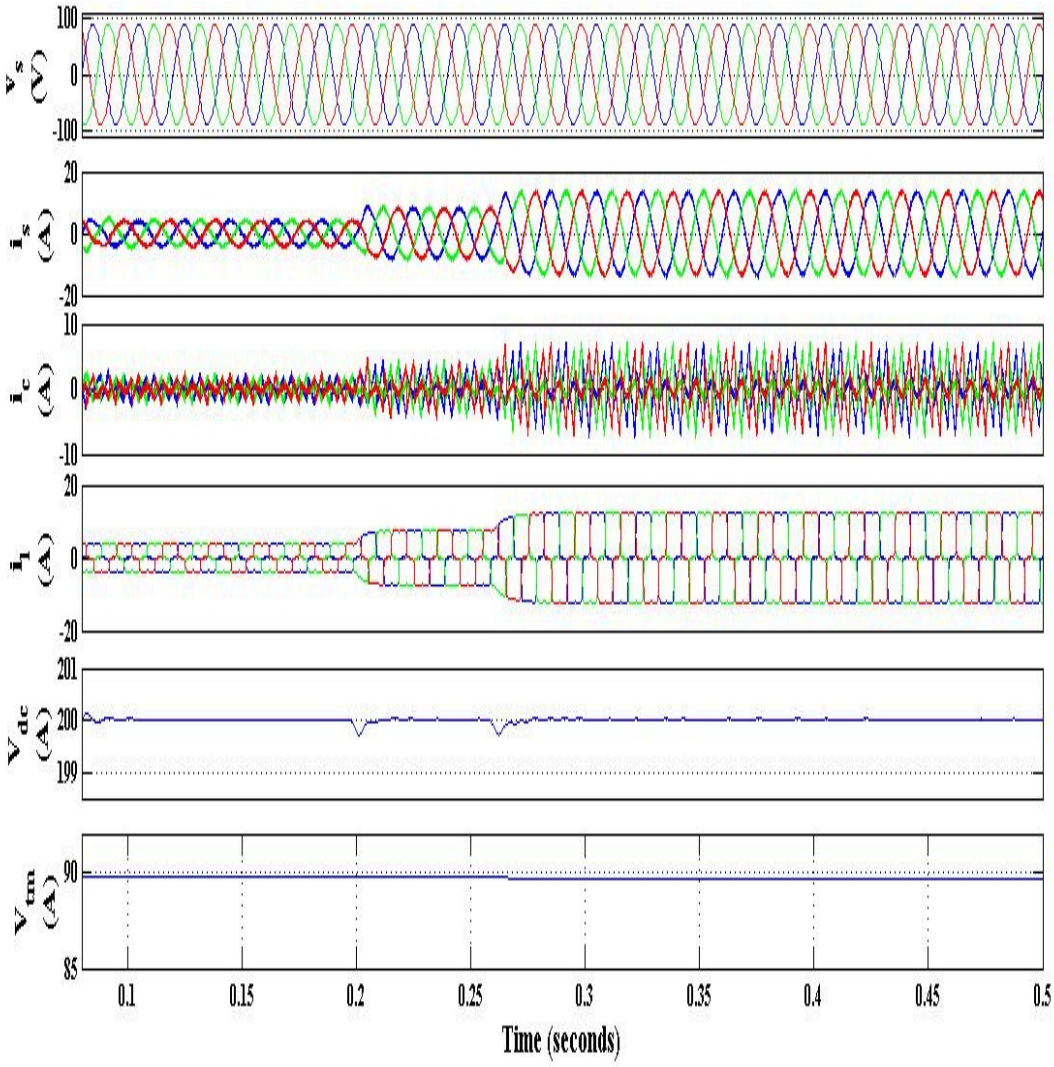

Fig. 3.12. Result showing source voltage (v_s), source current (i_s), compensator current (i_c), load current (i_l), DC link voltage (V_{dc}) and voltage at PCC (V_{tm}) under steady state / dynamic condition (UPF mode)

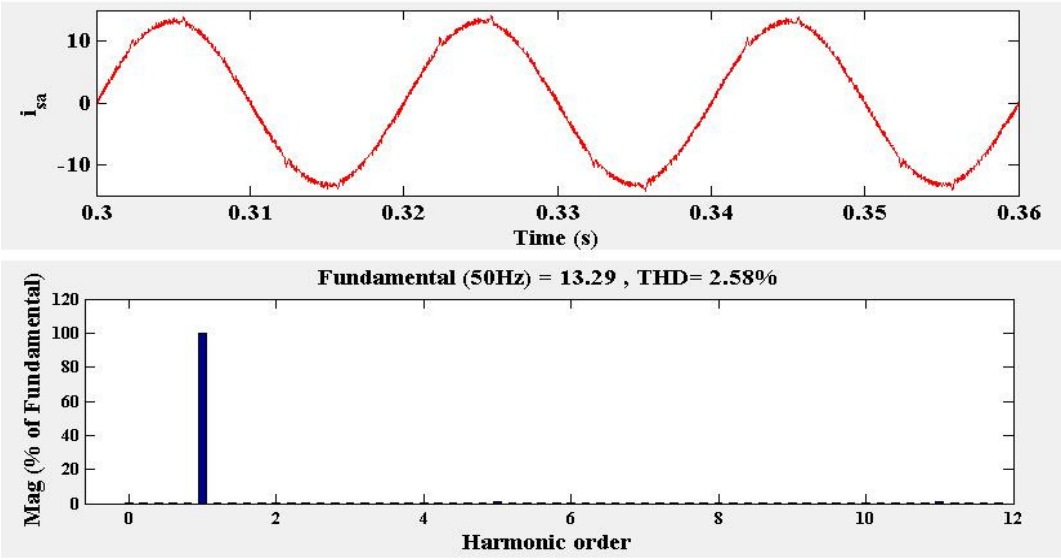

Fig. 3.13. Waveform and THD waveform of source current (i_{sa})

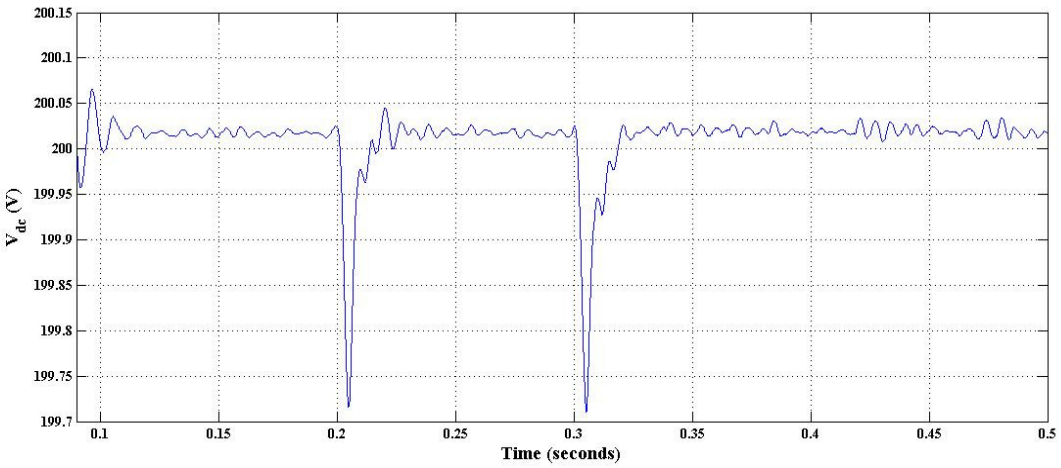

Fig. 3.14. Plot of DC link voltage (V_{dc}) with dynamic load changes with 25 rule FLC

3.4.3. FLC based on 9 rules

The fuzzy rules are partitioned into seven subsets that are N, Z, P for both the error (er) and change of error (Δer) input variables are shown in the Table 3. Fig 3.15 (a), (b) and (c) shows the membership function for input and output variables.

Table 3. Fuzzy logic controller rules for three rule base (9 rules)

Δer / er	**N**	**Z**	**P**
N	*N*	*N*	*Z*
Z	*N*	*Z*	*P*
P	*Z*	*P*	*P*

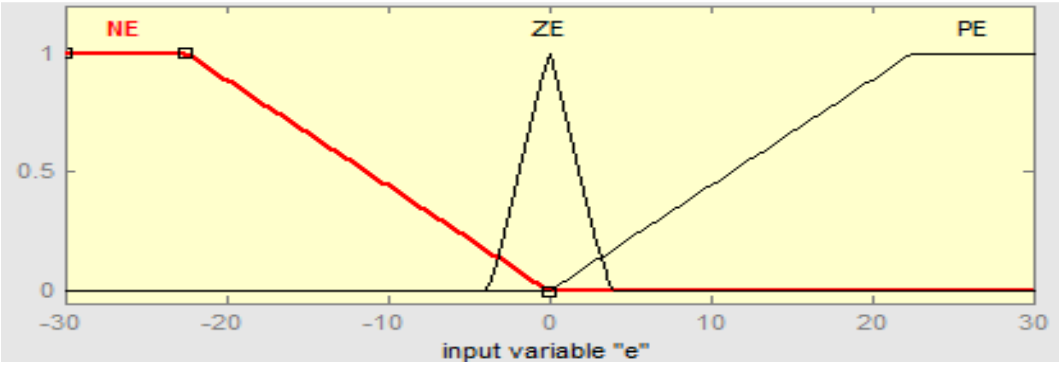

(a)

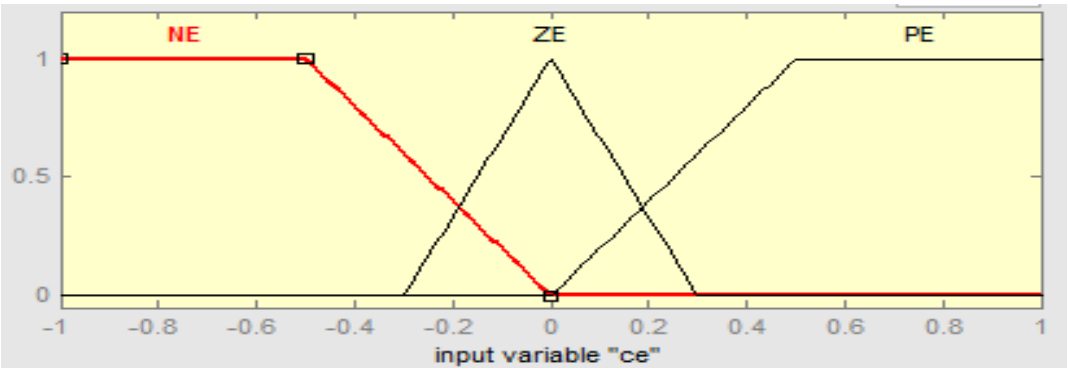

(b)

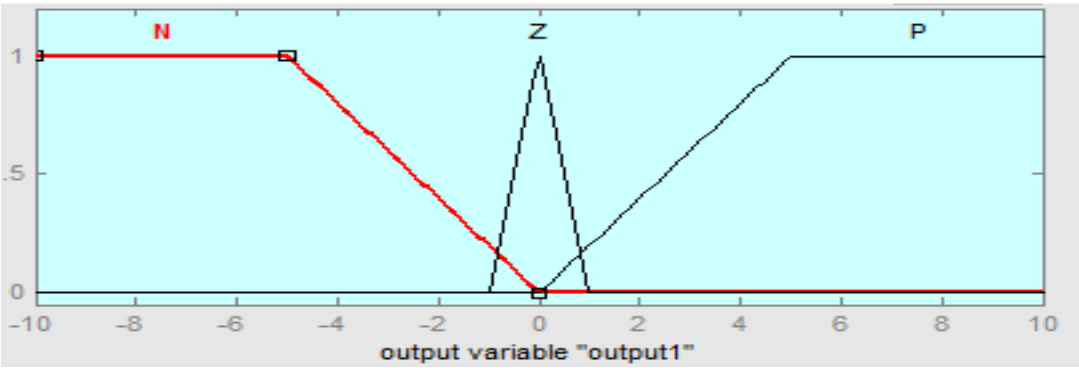

(c)

Fig. 3.15. FLC based on three rules (a) Input (er) (b) Input (Δer) (c) Output variables

3.4.3.1. Results for Power Factor improvement under steady state / dynamic conditions

Fig. 3.16 shows the waveforms of source voltage, source current, compensator current, load current, DC link voltage and voltage at PCC. It is observed that DC link voltage is maintained at reference value and PCC voltage is also regulated when load current is increased from 4A to 7.4A at t =0.2s and again increased to 12A at t=0.3s.

Fig. 3.17 shows the DC link voltage plot. It is seen that there slight increase in undershoot and overshoot voltage. When load current is increased at t= 0.2s and t=0.3s there is voltage dip which settles after small oscillations. Fig. 3.18 shows the THD waveform of source current which is 2.72%.

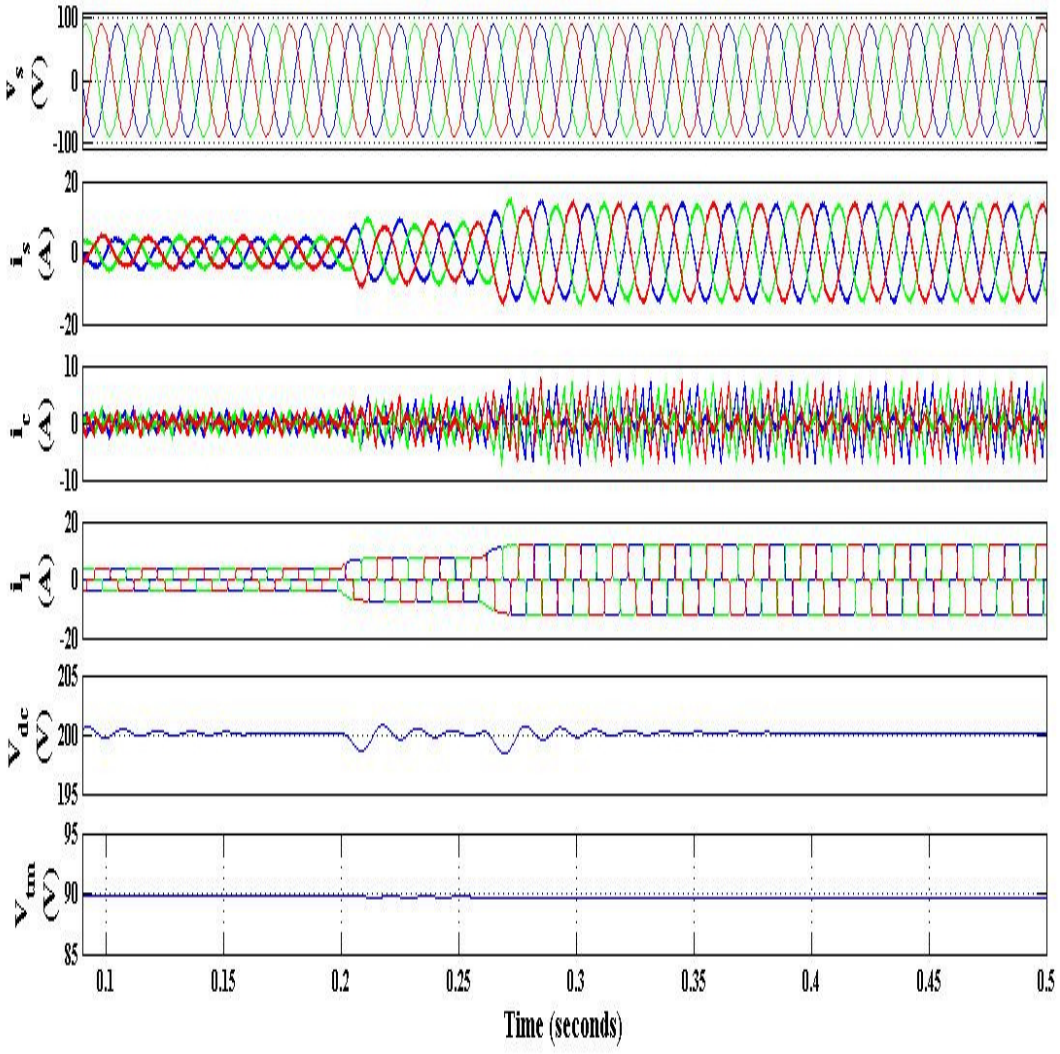

Fig. 3.16. Results of source voltage (v_s), source current (i_s), compensator current (i_c), load current (i_l), DC link voltage (V_{dc}) and voltage at PCC (V_{tm}) for power factor improvement under steady state/dynamic conditions

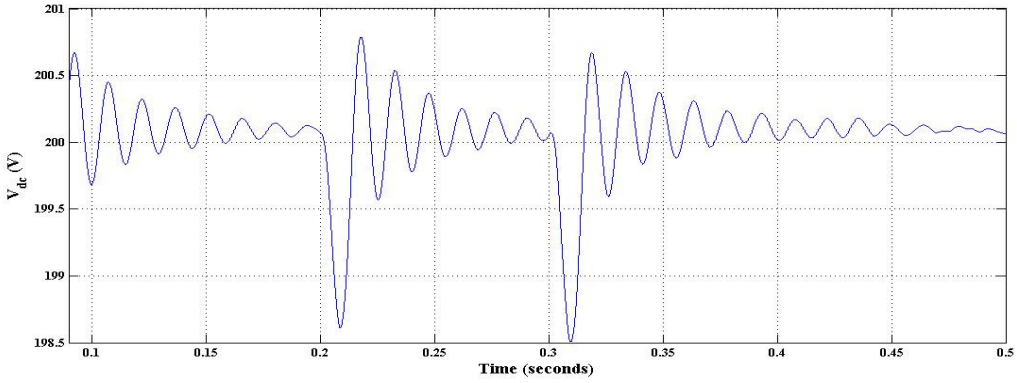

Fig. 3.17. DC link voltage (V_{dc}) plot under steady state / dynamic conditions

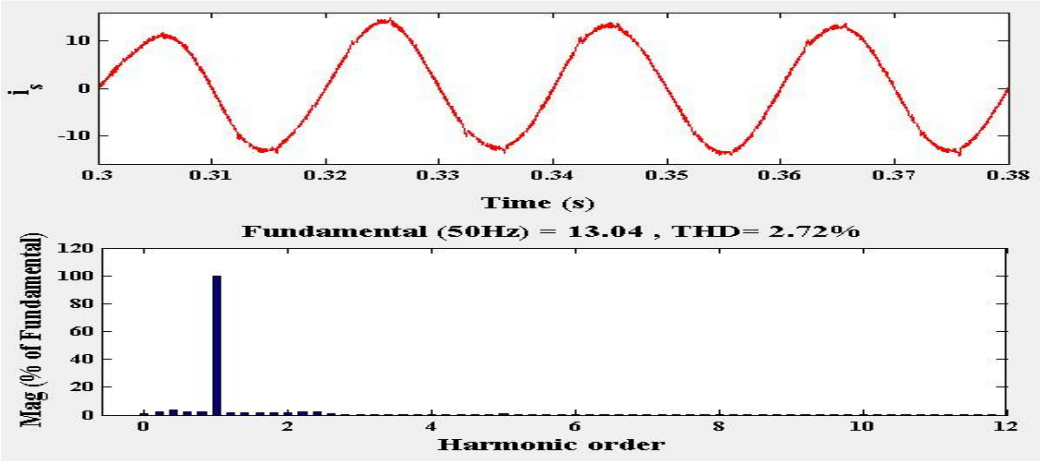

Fig. 3.18. Waveform and THD of source current (i_{sa})

3.5. Conclusion

Table 3.4 Comparative analysis of different fuzzy rules

Performance / Rules	THD of i_s (%)	Overshoot (max. V)	Undershoot (max. V)	Settling time (seconds)
49 rules	2.37	201.1	198.1	0.03
25 rules	2.58	201.4	197.85	0.04
9 rules	2.72	202.1	197.2	0.07

This chapter discusses in detail the design of fuzzy logic controller. Three designs have been considered with 49, 25 and 9 rules. The conventional PI controller in chapter 2 is replaced by FLC. Comparison is made for these on the basis of THD in source current, overshoot, undershoot and settling time. It is observed from the Table 3.4 that FLC performs better than PI controller in all cases. With 49 rules, overshoot is 201.1V and undershoot is 198.1V. With 25 rules, overshoot is 201.4 and undershoot is 197.85V. With 9 rules, overshoot is 202.1V and undershoot is 197.2V.

It is observed that performance with 25 rules is better than 49 rules while the performance with 9 rules is produces oscillation in DC link voltage. It is seen that all FLC controllers achieve IEEE 519 standards.

Chapter 4

Adaptive Neuro-Fuzzy based controller

4.1. General

Fuzzy controller has many applications in various industrial processes. In the previous chapter, the PI controller is replaced by fuzzy logic controller to get the loss component of the converter. Instantaneous active power theory involves the transformation of three phase quantity to two phase quantity and fails to work properly when voltages are distorted. SRF theory requires the filtering of the current to extract the dc component. In this chapter fuzzy logic controller (FLC) is used with neural network to extract the active component of the load current based on Adaline controller. The model has been simulated in MATLAB environment and also implemented on developed hardware prototype of D-STATCOM. The simulation and hardware model are discussed.

4.2. Step Size Variation in Adaline

In the conventional Adaline control algorithm constant step size is taken to update the weights to extract the positive sequence of the load current. For large step size, the convergence phenomenon is higher but stability error is more and if the step size is low, then the stability error will be less but convergence will be low. Therefore variable step size Adaline algorithm is used whose step size varies with time for updating weight and the weight varies as the load current changes. Here variable step size is obtained using fuzzy logic controller. Fig. 4.1 shows the block diagram of the conventional Adaline control scheme and Fig. 4.2 shows the block diagram Adaptive Neuro-fuzzy (ANFIS) algorithm for estimating the variable step size, where e_a, e_b and e_c are the error in load current of phase 'a', phase 'b' and phase 'c' & ce_a, ce_b and ce_c are the change in error in phase 'a', phase 'b' and phase 'c'.

Load current can be represented as shown in equation (4.1).

$$i_l = i_{p1} + i_{q1} + i_h \tag{4.1}$$

where, i_{p1}, i_{q1} and i_h fundamental active component, fundamental reactive component and harmonic component respectively.

The amplitude of PCC voltage is calculated from equation (4.2).

$$V_{tm} = \sqrt{\frac{2}{3}\left({v_{ta}}^2 + {v_{tb}}^2 + {v_{tc}}^2 \right)} \tag{4.2}$$

where, v_{ta}, v_{tb} and v_{tc} are terminal voltages at point of common coupling.

Unit vector templates in phase with PCC voltage are obtained from the equation (4.3).

$$u_a = \frac{v_{sa}}{V_{tm}} \quad ; \quad u_b = \frac{v_{sb}}{V_{tm}} \quad ; \quad u_c = \frac{v_{sc}}{V_{tm}} \tag{4.3}$$

Active component for single phase is calculated from equation (4.4).

$$i_p(n) = w_p(n) \times u_p(n) \tag{4.4}$$

According to LMS algorithm the weight should minimize the error in load current. The LMS iteration formula is shown in equation (4.5).

$$w_p(n+1) = w_p(n) + \Delta\mu\{i_l - (w_p(n) \times u_p(n))\} \times u_p(n) \tag{4.5}$$

where $w_p(n+1)$ is the updated weight, $w_p(n)$ is the current weight and $\Delta\mu$ is the step size which determines the convergence speed. Three phase active component of source current is calculated as shown in equation (4.6a), (4.6b) and (4.6c).

$$i_{sa}^{*}(n) = w_p(n) \times u_a(n) \tag{4.6a}$$

$$i_{sb}^{*}(n) = w_p(n) \times u_b(n) \tag{4.6b}$$

$$i_{sb}^{*}(n) = w_p(n) \times u_c(n) \tag{4.6c}$$

where the active component weight is calculated as shown in equation (4.7).

$$wp(n) = \frac{w_{pa}+w_{pb}+w_{pc}}{3} \tag{4.7}$$

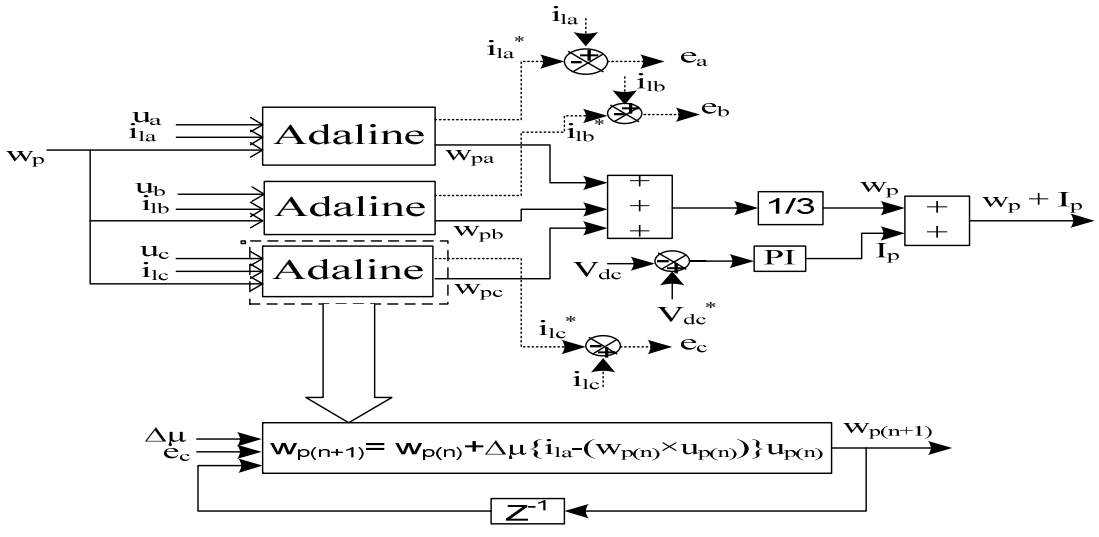

Fig. 4.1. Block diagram of ANFIS based on Adaline algorithm

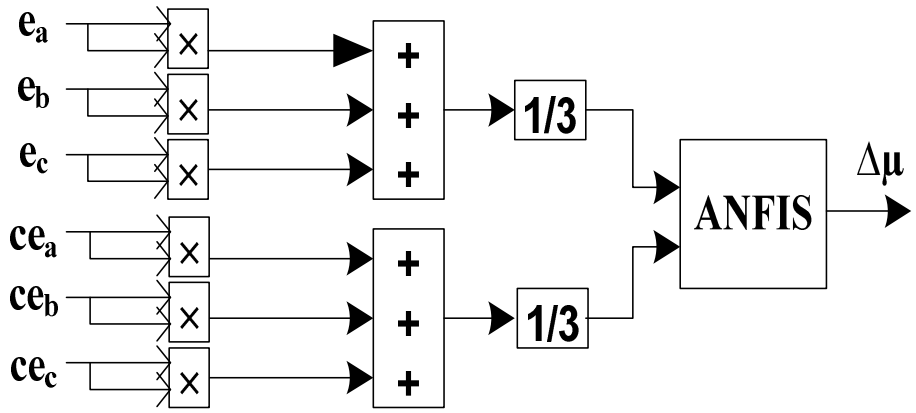

Fig. 4.2. Block Diagram of Adaptive Neuro-Fuzzy for estimating variable step size

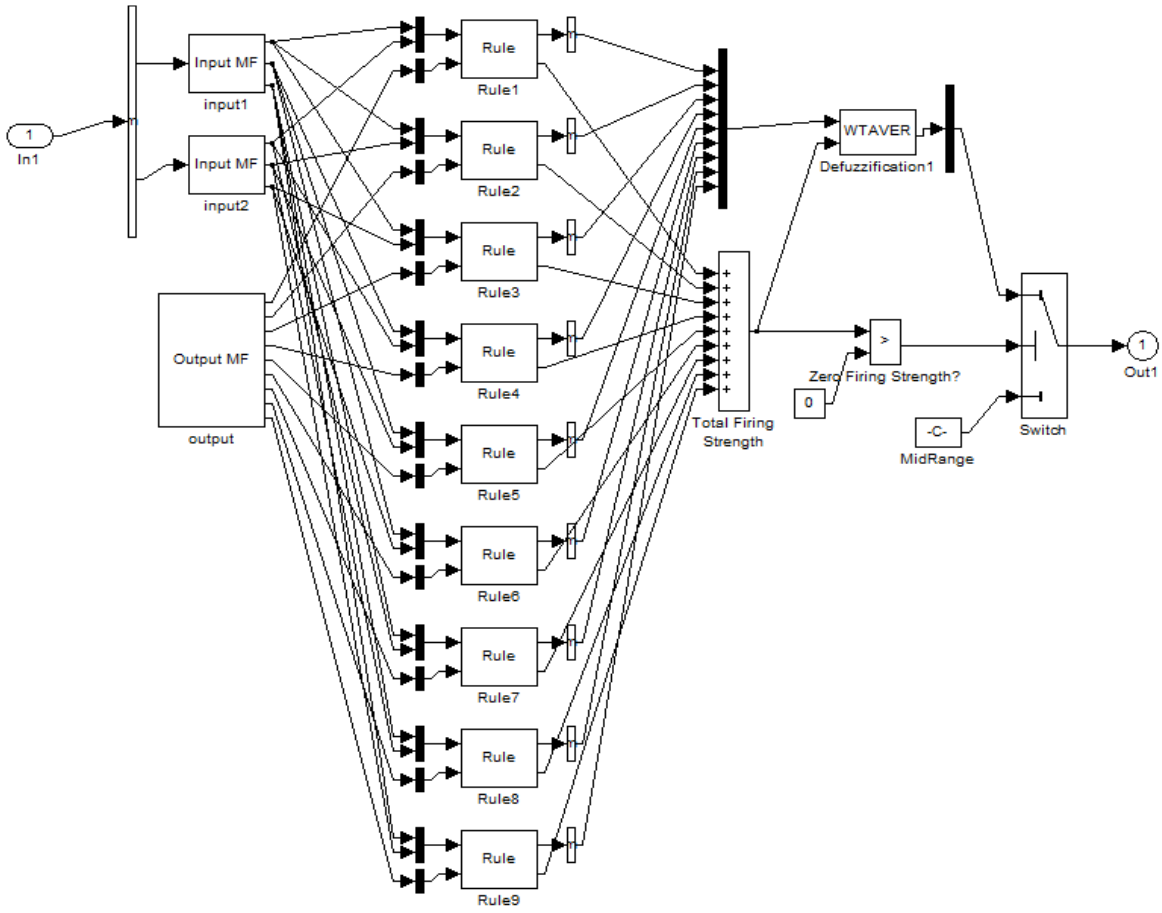

Fig. 4.3. Adaptive Neuro-Fuzzy rules (9 rules)

Adaptive neuro-fuzzy method is used for formulation of fuzzy rules which are trained by neural network using ANFIS editor in MATLAB environment. Triangular waveform is used as membership function. Simulation results and hardware results are shown in the next section.

4.3. Simulation results

Fig. 4.4. shows the waveform of source voltage, source current, compensator current, load current, DC link voltage, PCC voltage. It can be seen from the plot that the DC bus voltage is maintained at reference value which is 200V. Under unbalance condition when phase 'a' is removed at t = 0.3s, then there is rise in DC bus voltage which is quite high as shown in the plot. DC bus voltage is settled to reference voltage again. Then phase 'a' is again added at t = 0.5, then there is dip in the voltage which is again quite high but this reference voltage settles to reference voltage after very few cycles. The source current is found to be sinusoidal and harmonic free.

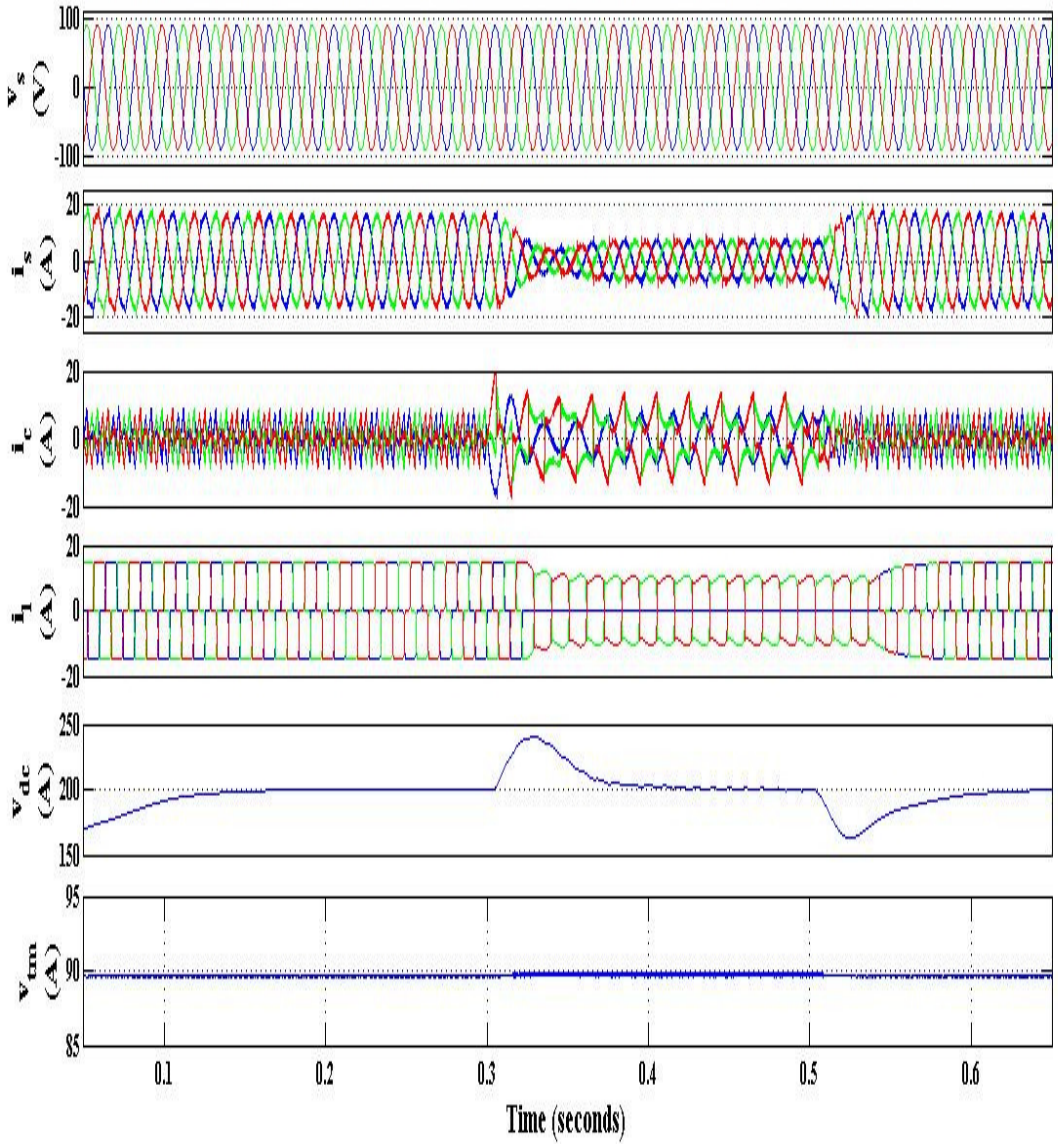

Fig. 4.4. Waveforms of source voltage (v_s), source current (i_s), compensator current (i_c), load current (i_l), DC bus voltage (V_{dc}) and terminal voltage (V_{tm}) under steady state and unbalance conditions

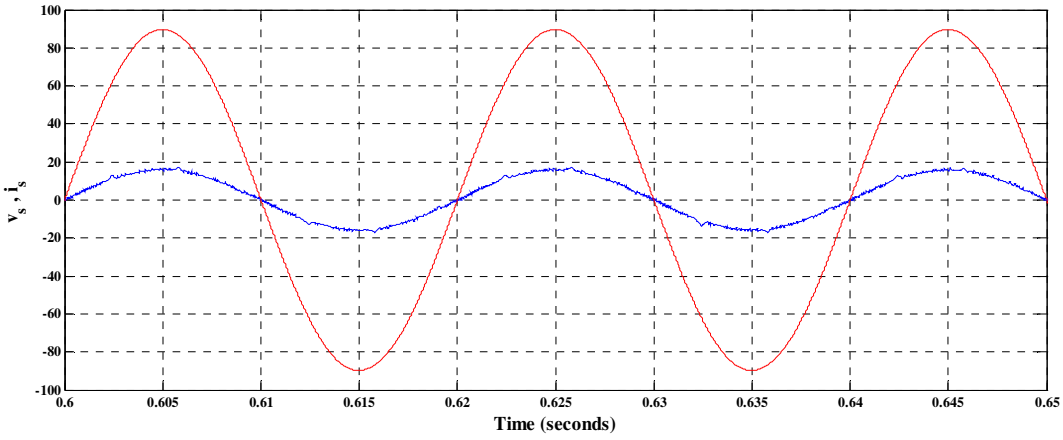

Fig. 4.5. Plot for source voltage (v_{sa}) and source current (i_{sa})

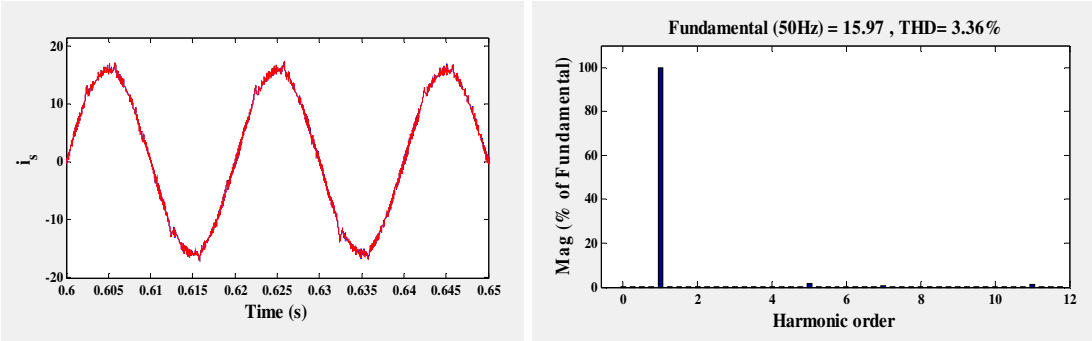

Fig. 4.6. Waveform and THD of source current (i_{sa})

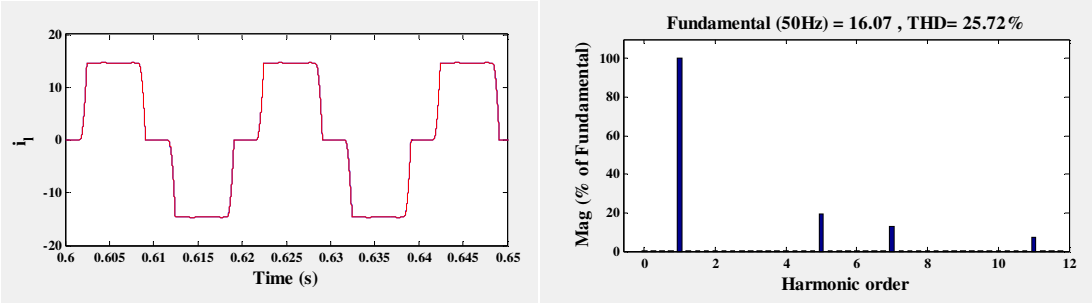

Fig. 4.7. Waveform and THD of load current (i_{la})

Fig. 4.5 shows the plot for source voltage and source current and it can be seen that source voltage and current are in phase with each other sowing unity power factor. Fig. 4.6 shows the THD of source current which is 3.36%. Fig. 4.7 shows the THD of load current which is 25.72%.

4.4. Hardware results

The simulation model has been implemented in hardware prototype of D-STATCOM. The hardware parameters are mentioned in appendix A. These results are taken through

fluke three phase Power Analyser. Fig. 4.8 shows the three phase supply voltage. it is observed that there is an unbalancing in the supply voltage and THD of source voltage is 4.8% which is shown in the Fig. 4.9.

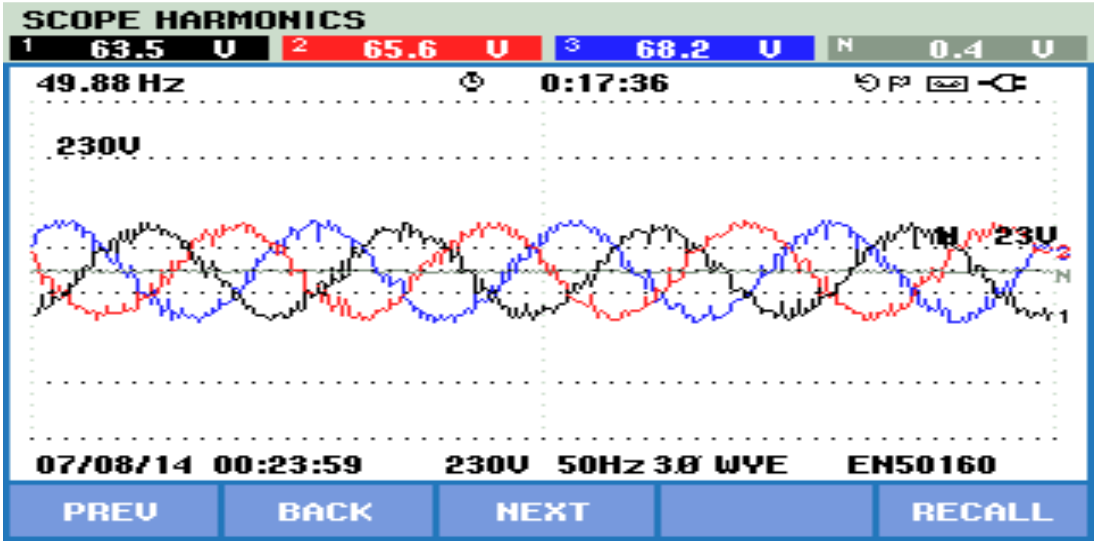

Fig.4.8. Three phase source voltage (v_s) waveform

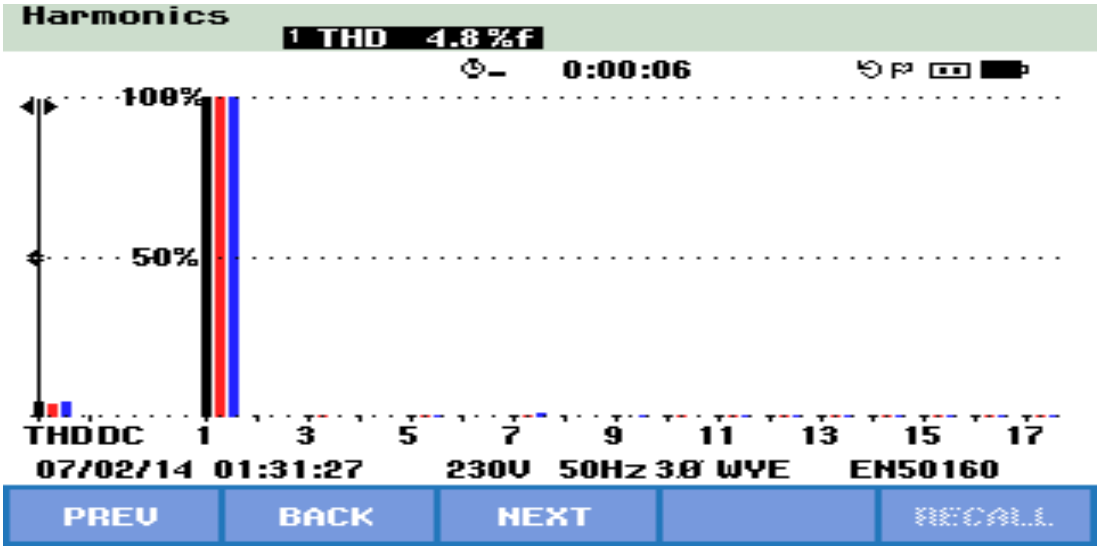

Fig.4.9. THD of source voltage (v_s)

Fig. 4.10 shows the waveform of three phase source current and corresponding THD is shown in Fig. 4.11 which is 7.4%. Fig. 4.12 shows three phase load current waveform. THD of load current is 24.8%, which is shown in Fig. 4.13.

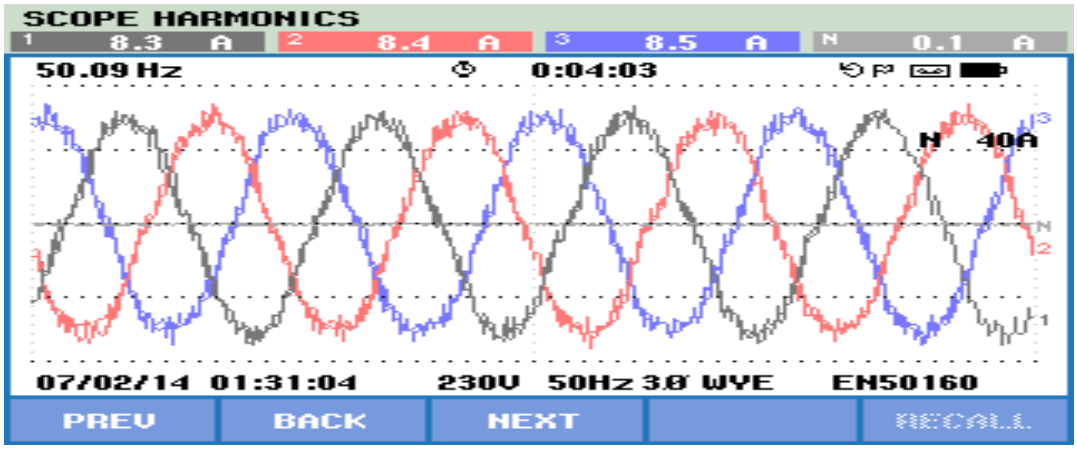

Fig.4.10. Three phase source current (i_s) waveform

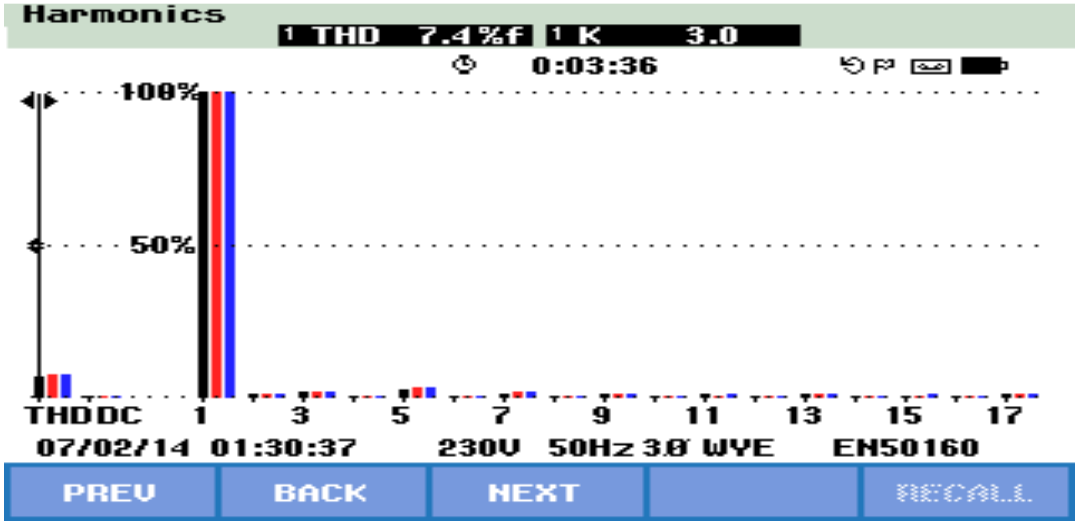

Fig. 4.11. THD of source current (i_s)

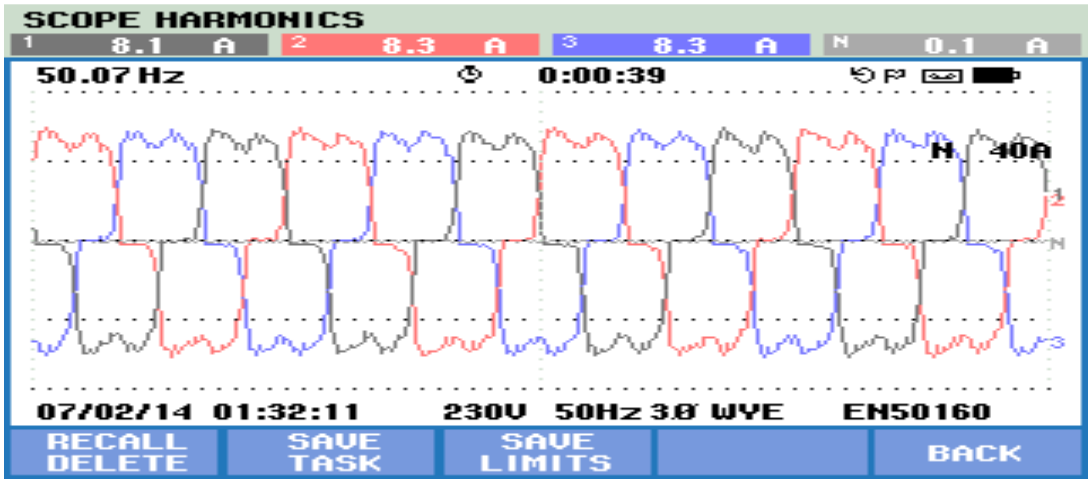

Fig. 4.12. Three phase load current (i_l) waveform

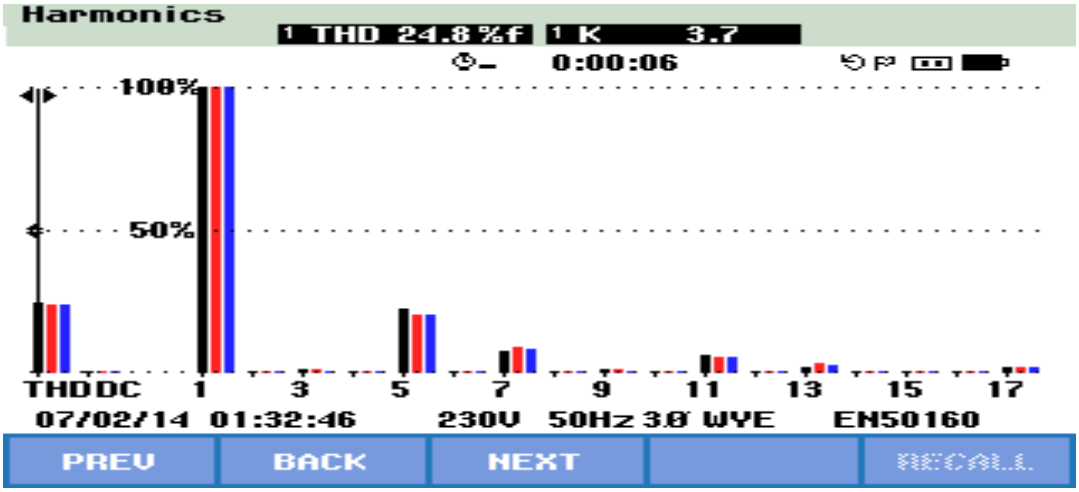

Fig. 4.13. THD of Load current (i_l)

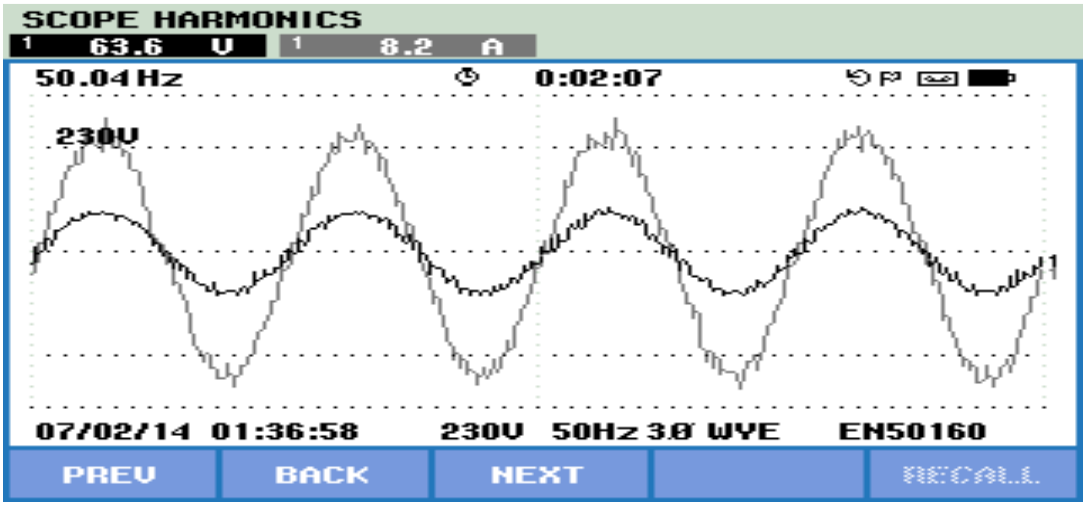

Fig. 4.14. Plot of source voltage (v_{sa}) and source current (i_{sa})

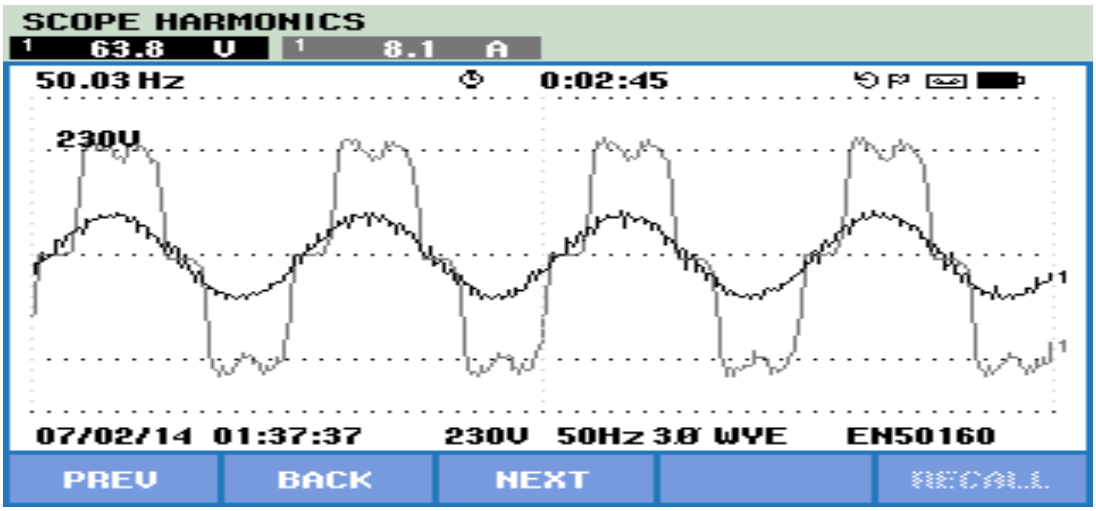

Fig. 4.15. Plot of source voltage (v_{sa}) and load current (i_{la})

Fig. 4.14 shows the source current and source voltage waveform and it is observed that the source voltage and source current are in phase with each other showing unity power factor operation. Fig. 4.15. shows the plot of source voltage and load current.

4.5. Conclusion

In this chapter, a variable step size Adaline is developed base on Adaptive Neuro-fuzzy (ANFIS) to extract the active component of load current. The model has been simulated in MATLAB environment and also implemented on hardware prototype of D-STATCOM. The simulation results showed that THD of the source current is 3.36%, while THD of load current is 25.72%. The developed control algorithm improves the power factor to unity. It takes long time to settle DC link voltage to its reference value. At the instant of unbalance, when load is removed from the phase then there is high rise in the DC link voltage and when load is added to the phase, there high dip in DC link voltage.

The hardware results showed that the control algorithm improves the power factor to unity. The THD of the source current is 7.4%, when THD of source voltage is 4.8% and THD of load current is 24.8%.

CHAPTER 5
CONCLUSION AND FUTURE WORK SCOPE

5.1. Conclusion

In this thesis work, conventional control algorithms i.e. Synchronous reference Frame theory (SRFT) and Power Balance Theory (PBT) have been simulated in MATLAB environment. The results showed that these conventional algorithms work effectively for compensating harmonic, reactive power and unbalancing in load. The PBT algorithm has been implemented and results compared with simulation results. Hardware results are also presented with non linear load for power factor improvement. It is observed that THD of the source current is found to be less than 5% as per IEEE 519 standard.

In conventional algorithm, PI controller is used for extracting the loss component in the converter. PI controller has some disadvantages as it requires fixed value of proportional and integral gain. It also gives unsatisfactory result if system condition or parameter changes occur. Therefore an automatic controller is required to that can change the gain value depending on system conditions. For this, PI controller is replaced by Fuzzy Logic Controller (FLC). Different fuzzy rule sets of 49 rules, 25 rules and 9 rules are formulated and simulated in MATLAB environment. It is observed that FLC with 25 rules give more satisfactory results and improves the DC link response. It is found that THD of the source current is less than 5% as specified by IEEE standards.

In Fuzzy Logic Controller (FLC), the computational time is very high, therefore it is difficult to implement on hardware prototype. Therefore Adaptive neural network algorithm based Adaline controller is developed in MATLAB environment and implemented on hardware prototype of D-STATCOM. It is observed from the simulation results that the THD of source current is found to be less than 5% and also the power factor of the source current is improved to unity. But under unbalanced condition, when load is removed / added, there is a rise /dip in DC link. The hardware results shows that THD of the source current is 7.4% , whereas the THD of source voltage is 4.8% for the load current THD of 24.8%.

This thesis focuses on a few conventional algorithms for control of D-STATCOM and also investigates the use of Fuzzy logic based and neural network based control algorithms. With FLC controller, the overshoot and undershoot in DC link voltage is very small even under dynamic load changes and phase removal of load. The use of

ANFIS is new and promising controller and can be successfully designed for power quality improvement. Both these controllers perform better than the PI controller and the need to optimize the PI gain constants can be eliminated.

5.2. Future scope of work

1. Variable step size Adaline controller need further improvements to reduce the THD of the source current. The hardware results show that the source voltage have high THD of 4.8% and hence the THD obtained in source current is 7.4%. hence the supply voltages need to be filtered first and then used in design of ANFIS based Adaline controller for better results.
2. Implementation of fuzzy controller can be taken up in future.
3. Only three-phase three-wire D-STATCOM structure has been studied. Some other configuration can be studied in future.

REFERENCES

[1]Government of India, Central Electricity Authority, Ministry of Power (www.mnre.gov.in)

[2]Mohan, Undeland, Robbins, "Power electronics:converter, application and design".

[3]B.K Bose, Power Electronics and AC Drive, Prentice Hall.

[4]Angelo Baggini, "Hand Book on power quality,"John Wiley &Sons, New Jersy, USA, 2008.

[5]C. Sankaran, *Power Quality*. Boca Raton, FL: CRC Press, 2002.

[6]"Power Quality Primer", The McGraw-Hill.

[7]Roger C. Dugan, Mark F. McGranaghan, Surya Santoso and H.Wayne Beaty, "Electrical Power Systems Quality", The McGraw-Hill, Second Edition, 2004.

[8]Arindam Gosh and Gerard Ledwich, " power quality enhancement using custom power devices".

[9]Power System Harmonics J Amiag, edition John Wiley & Sons.

[10] M. Bollen, "Understanding Power Quality Problems – Voltage Sags and Interruptions", IEEE Press Series on Power Engineering – John Wiley and Sons, Piscataway, USA (2000).

[11] J.C. Das, "Passive filters - potentialities and limitations," *Industry Applications, IEEE Transactions on*, vol. 40, pp. 232-241, 2004.

[12] N.G. Hingorani, "Introducing custom power," *Spectrum, IEEE*, vol. 32, pp. 41-48, 1995.

[13] Hurfumi Agaki, Edson Hirokazu watanabe, Mauricio Aredes, "instantaneous power theory and application to power conditioning".

[14] H. Agaki, Y Kanazawa and A. Nabae, " Generalized theory of the instantaneous reactive power in three phase circuit," *in Proc. IEEE IPEC, 1983, pp. 821-827*.

[15] H. Fujita and H. Akagi, "Voltage-regulation performance of a shunt active filter intended or installation on a power distribution system," *IEEE Trans. Power Electron.*, vol. 22, no. 3, pp. 1046–1053, May 2007.

[16] C.L. Chen, C.E. Lin, C.L. Huang, "An active filter for unbalanced three-phase system using synchronous detection method", *IEEE-PESC Conf.*, pp 1451–1455, 1994.

[17] B. Singh, K. Al-Haddad, and A. Chandra, "A review of active filters for power quality improvement," *Industrial Electronics, IEEE Transactions on*, vol. 46, pp. 960-971, 1999.

[18] B. Singh, A. Adya, A. P. Mittal, J. R. P. Gupta, "Modeling, design and analysis of different controllers for DSTATCOM", *Joint International Conference on Power System Technology POWERCON and IEEE Power India Conference, POWERCON 2008.*

[19] B. Singh, K. Al-Haddad, and A. Chandra, "A new control approach to three-phase active filter for harmonics and reactive power compensation," *IEEE Trans. on Power Systems*, vol. 13, no. 1, pp. 133–138, Feb. 1998.

[20] B.N. Singh, B. Singh, A. Chandra and K. Al-Haddad, "Design and digital implementation of active filter with power balance theory," *IEEE Proc.-Electr. Power Applications,* vol. 152, no. 5, pp. 1149-1160, September 2005.

[21] B.N. Singh, B. Singh, A. Chandra, P. Rastgoufard and K. Al-Haddad, "An Improved Control Algorithm for Active Filters," *IEEE Trans. On Power Delivery*, vol. 22, pp. 1009-1020, April 2007.

[22] B. Singh, V. Verma, A. Chandra and K. Al-Haddad, "Hybrid Filters for Power Quality Improvement", IEEE Proc. Generation, Transmission and Distribution", Vol.152, Page(s): 365 - 375, 2005.
[23] B. Singh and V. Verma, "An indirect current control of hybrid power filter for varying loads," *IEEE Trans. Power Del.*, vol. 21, no. 1, pp. 178–184, Jan. 2006.
[24] Y. Li, K. H. Ng and G. C. Y. Chong, "PID Control System Analysis and Design", IEEE Control Systems Magazine 26(1): 2004, pp. 32-41.
[25] Yaow-Ming **Chen,** Robert M. O'Connell, "Active Power **Line** Conditioner with a Neural Network Control", IEEE Trans. Ind. AppliCation~~, 01.33p, p.1131-1136, July/AuguSt 1997.
[26] B. Widrow, J. M. McCool, M. G. Larimore, and C. R. Johnson, "Stationary and nonstationary learning characteristics of the LMS adaptive filter," ***Proc. IEEE,*** vol. 64, pp. 1151-1162, Aug. 1976.
[27] B. Widrow, **J.** R. Glover, Jr., J. M. McCool, J. Kaunitz. C. **S.** Williams, R. H. Hearn. I. R. Zeidler, E. Dong, **Jr.,** and **R.** C. Goodlin, "Adaptive noise cancelling: Principles and applications, " ***Proc. IEEE,*** vol. 63. pp. 1692-1716, Dec. 1975.
[28] B. Singh, V. Vishal and J. Solanki " Active power filter selective compensation of current using neural network" in Proc. of IEEE ISIE'04, May 2004.
[29] B. Singh, V. Vishal, J. Solanki, A. Chandra and K. Al Haddad "Neural network controlled power conditioner with battery energy storage feature for isolated offshore power system" in Proc. of IEEE PCI'04 Nov. 2004. Pp 127-133.
[30] Singh, J. Solanki, and V. Verma, " Neural Network Based Control of Reduced Rating DSTATCOM," *in proc. Of IEEE-INDICON, 2005, pp. 516-520.*
[31] S. Karanki, N. Geddada, Mahesh K. Mishra, and B. Kumar, "A DSTATCOM topology with reduced dc-link voltage rating for load compensation with nonstiff source," *IEEE Trans. Power Electron*, vol. 27, no. 3, pp. 1201–1211, Mar. 2012.
[32] Mikkili Suresh, Panda AK. PI and fuzzy logic controller based 3-phase 4-wire shunt active filter for mitigation of current harmonics with Id–Iq control strategy. J Power Electron (JPE) (KIPE – South Korea) 2011;11(6):914–21.
[33] Vijay B. Bhavaraju and Prasad N. Enjeti, "An Active line Conditioner to Balance Voltages in a Three-Phase System", *IEEE Trans. on Ind. Appl.*, vol. 32, N°2, March./April 1996.
[34] S. Bhattachrya, D. Divan, "Synchronous Frame based controller implementation for a hybrid series active filter systems", *IEEEIAS Annual Meeting,* pp 2531–2540, 1995.
[35] NIELSEN J.G., BLAABJERG F., MOHAN N.: 'Control strategies for dynamic voltage restorer compensating voltage sags with phase jumps'. Proc. IEEE APEC'01, 2001, vol. 2, pp. 1267–1273
[36] GHOSH A., JINDAL A.K., JOSHI A.: 'Design of a capacitor supported dynamic voltage restorer (DVR) for unbalanced and distorted loads', IEEE Trans. Power Deliv., 2004, 19, (1), pp. 405–413
[37] WEI LI Y., MAHINDAV., BLAABJERGF., CHIANG LOHP.: 'A robust control scheme for medium-voltage-level dvr implementation', IEEE Trans. Ind. Electron., 2007, 54, (4), pp. 2249–2261.
[38] NEWMAN M.J., HOLMES D.G., NIELSEN J.G., BLAABJERG F.: 'A dynamic voltage restorer (DVR) with selective harmonic compensation at medium voltage level', IEEE Trans. Ind. Appl., 2005, 41, (6), pp. 1744–1753.

[39] D. M. Divan, S. Bhattacharya, and B. Banerjee, "Synchronous frame harmonic isolator using active series filter," in *Proc. Eur. Power Electron.Conf.*, 1991, pp. 3030–3035.
[40] B.Singh and V.Verma, "Selective Compensation of Power-quality problems Trrough Active Power Filter by Current Decomposition,"IEEE Trans. On Power Delivery,vol.23,No.2,pp.792-799,April 2008.
[41] B.Singh and Venkateswarlu, "A Simplified Control Algorithm for Three-Phase Four-Wire Unified Powe Quality Conditioner," Journal of *Power Electronics*, vol.10, No.1, January2010.
[42] IEEE 519-1992 standard IEEE Recommended practices and requirement for harmonic control in electrical power system.
[43] IEC-555 Disturbances in supply system caused by household appliances and similar electrical equipments.
[44] IEEE 1159-1995 standard IEEE Recommended practices for monitoring electric power quality.
[45] B. K. Bose, "An adaptive hysteresis-band current control technique of a voltage-fed PWM inverted for machine drive system," *IEEE Trans. Ind. Electron*., vol. 37, pp. 402–408, Oct. 1990.
[46] T. W. Chun and M. K. Choi, "Development of adaptive hysteresis band current control strategy of PWM inverter with constant switching frequency," in *Proc. IEEE APEC'96*, San Jose, CA, pp. 194–199, 1996.
[47] D. Abramovitch, "Some crisp thoughts on fuzzy logic," *American Control Conference*, Vol. pp. 168-172, 1994.
[48] Saad S, Zellouma L. Fuzzy logic controller for three-level shunt active filter compensating harmonics and reactive power. Electr Power Syst Res 2009;79:1337–41.

APPENDIX

Parameters of the proposed distribution network system in simulations and hardware:

Sl. No.	Parameters	Value
1	Line to line rms source voltage	110V
2	System frequency (f)	50 Hz
3	Source impedances	$R_s = 0.1\Omega$
		$L_s = 0.5mH$
4	Interfacing Filter impedance	$R_c = 0.2\ \Omega$, $L_c = 3.2mH$,
5	3-phase diode rectifier load	$R = 18\text{-}60\Omega$
		$L = 100mH$
6	Proportional Gain, K_p	0.35
7	Integral Gain, K_i	0.001
8	Capacitance of DC link capacitor	1640μF

PUBLICATIONS

Published

[1] Nitu Dhyani, Alka Singh and Manoj Badoni, "'Implementation of Distribution Energy Source as a Compensator based on Power Balance Control Algorithm", in International Conference on Signal Propagation and Computer Technology (ICSPCT)-2014 at Govt. Engineering College Ajmer, India, Technical Sponsored by IEEE Delhi Section.